Available online at www.sciencedirect.com
SCIENCE DIRECT®
Icarus 174 (2005) 535–559
ICARUS
www.elsevier.com/locate/icarus

South polar residual cap of Mars: Features, stratigraphy, and changes

P.C. Thomas [a,*], M.C. Malin [b], P.B. James [c], B.A. Cantor [b], R.M.E. Williams [b], P. Gierasch [a]

[a] *Center for Radiophysics and Space Research, Cornell University, Ithaca, NY 14853, USA*
[b] *Malin Space Science Systems, P.O. Box 910148, San Diego, CA 92191, USA*
[c] *Department of Physics and Astronomy, University of Toledo, Toledo, OH 43606, USA*

Received 8 March 2004; revised 13 July 2004

Available online 1 February 2005

Abstract

The south residual polar cap of Mars, rich in CO_2 ice, is compositionally distinct from the north residual cap which is dominantly H_2O ice. The south cap is also morphologically distinct, displaying a bewildering variety of depressions formed in thin layered deposits, which have been observed to change by scarp retreat over an interval of one Mars year (Malin et al., 2001, Science 294, 2146–2148). The climatically sensitive locale of the residual caps suggests that their behavior may help in the interpretation of recent fluctuations or repeatability of the Mars climate. We have used Mars Global Surveyor Mars Orbiter Camera (MOC) images obtained in three southern summers to map the variety of features in the south residual cap and to evaluate changes over two Mars years (Mars y). The images show that there are two distinct layered units which were deposited at different times separated by a period of degradation. The older unit, ~ 10 m thick, has layers approximately 2 m thick. The younger unit has variable numbers of layers, each ~ 1 m thick. The older unit is eroding by scarp retreat averaging 3.6 m/Mars y, a rate greater than the retreat of 2.2 m/Mars y observed for the younger unit. The rates of scarp retreat and sizes of the different types of depressions indicate that the history of the residual cap has been short periods of deposition interspersed with longer erosional periods. Erosion of the older unit probably occupied ~ 100–150 Mars y. One layer may have been deposited after the Mariner 9 observations in 1972. Residual cap layers appear to differ from normal annual winter deposits by having a higher albedo and perhaps by having higher porosities. These properties might be produced by differences in the depositional meteorology that affect the fraction of high porosity snow included in the winter deposition.

Keywords: Mars; Poles; Atmosphere; Climate

1. Introduction

A southern residual cap on Mars has been observed telescopically for more than a century (Flammarion, 1892). Maraldi observed that the south polar cap was offset from the geographic pole as early as 1720, and Schiaparelli found a displacement of the residual cap consistent with modern values (Flammarion, 1892). Although there have been reports of its disappearance (Lowell, 1895; Kuiper, 1957), these claims were not confirmed and may have been due to obscuration by dust events (Slipher, 1962). Mariner 9 provided the first detailed spacecraft images of the martian polar caps, with pixel scales as good as 95 m. Comparison of Mariner 9 images taken in 1972 with those obtained by Viking in 1977 showed many areas of the residual cap which were dark in Mariner 9 summer images were relatively bright in Viking data, giving a more variegated and slightly less extensive appearance to the earlier views (James et al., 1979, 1992). Thermal data obtained by Viking indicate a dominantly CO_2 composition of the south residual cap, as does the minimal water detection (Kieffer, 1979; Paige et al., 1990). By contrast, the northern residual cap is firmly identified as water ice (Kieffer et al., 1976). MOC images of a few m/pixel showed that the southern residual cap also has a morphology that is totally different from that in the north (Fig. 1) (Thomas et al., 2000) and which has an impressive variety of depressions and layer expo-

* Corresponding author.
E-mail address: thomas@baritone.astro.cornell.edu (P.C. Thomas).

0019-1035/$ – see front matter
doi:10.1016/j.icarus.2004.07.028

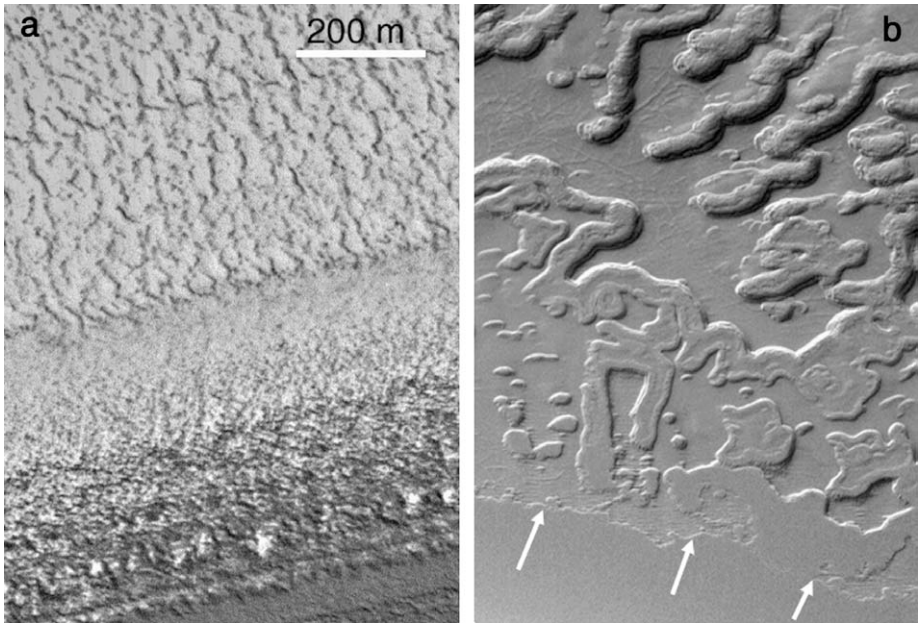

Fig. 1. Comparison of north and south residual caps at the same scale. Left is north residual cap grading into layers of the main polar layered deposit. MOC image M00-02072, 86.0° N, 258.1° W, $L_s = 137°$, nazim = 313°. Right, south residual cap, showing very different topography from that in the north, and the sharp margin (arrows) of the residual cap layers on the main layered deposit. This is a prominent contrast to the gradational contact in the north. MOC image M07-02129, 86.9° S, 77.8° W, $L_s = 43°$, nazim = 252°.

sures. After two Mars southern summers of observations, the high-resolution MOC images showed that the few-meter high scarps in the south residual cap had retreated about 3 m (Malin et al., 2001). The retreat suggested a net loss of CO_2 from the residual cap, either to the atmosphere or into regolith sites. Infrared spectral mapping from Mars Express Orbiter at ~ 2 km scales has detected CO_2 ice in the bright areas of the residual cap, and H_2O ice in some of the darker areas (Bibring et al., 2004). The character of the spectra indicates that in some areas there is intimate mixing of the two ices. The findings confirm the basic character of the residual cap as CO_2, and suggest it is underlain by water ice rich materials. Although there is something of a CO_2 reservoir at the south pole (Leighton and Murray, 1966), the situation is probably different from the deep buffer they proposed.

This paper presents a study of the south polar residual cap morphology based primarily on MOC image data. We first review the data and methods employed. Then we summarize the types of features observed and their basic stratigraphic relations. This is followed by examination of two Mars y of changes seen in MOC images for the various types of features found in the residual cap. Changes on the longer time scale between Mariner 9, Viking, and MOC are then briefly reported. Then follow sections analyzing the likely development of the residual cap deposits, their degradation, and the possible causes of the changing conditions in the cap area. We conclude with a summary of some of the unsolved problems.

We follow the common terminology of "polar layered deposits," or PLD, as referring to the large stacks of material, probably containing both water ice and silicate dust, that occur at both poles. In at least the southern example, they are distinct from the overlying residual cap materials.

2. Methods

We examined the morphology of the south residual cap in several hundred MOC images of 1.5–11 m pixel scales. Line and sample coordinates of several types of erosional depressions and layer exposures were digitally recorded from raw images. These coordinates were converted to latitude and longitude, and size and orientation, by spherical trigonometric scaling from corner coordinates supplied by Malin Space Science Systems software. Absolute location errors may be of order a km, but uncertainties of size within an image are largely due to range uncertainties, perhaps ~ 1% from assumption of a topographic model surface. Changes in feature dimensions were derived by measurement of distinctive parts of depressions, septa, or other features that could be reliably marked in images with slightly different lighting. Errors in these relative measures are essentially all due to digitizing, as scale errors induced by assumptions of planetary radius apply equally to each observation. Images were specifically targeted to repeat those obtained one or two Mars y previously within a few degrees of L_s in order to have lighting and albedo as similar as possible. Thicknesses of layers were determined with shadow measurements in images of 1.5–3 m pixel scales and incidence angles greater than 65° (incidence is angle from the normal). Heights of mesas of sufficient extent were recorded from overlaid tracks of Mars Orbiter Laser Altimeter (MOLA) data. MOLA grid-

ded data were used for characterization of the altitude and regional slope characteristics of the different mapped features.

MOC images are numbered by mission segment, month, and consecutive image number. In this paper we use data from the mapping (M; 1999 and early 2000 for images used here) orbits, extended mission (E; largely 2001) orbits, and relay mission (R; 2003) orbits. Image numbers are thus of the form M03-02089 for image 2089 from the 3rd month of the mapping mission. The narrow and wide angle cameras are referred to as NA and WA, respectively. Seasons are given by the aerocentric longitude of the Sun, L_s, where 0° is the start of northern spring. All MOC narrow angle images presented here are portions of the original frames, and all have been contrast enhanced. MOC narrow angle images are shown with illumination from the lower right unless otherwise indicated. In the figure captions, nazim is the angle, clockwise from up, of north.

3. Morphologic features of the south polar residual cap

3.1. Overview

The almost fantastic array of forms on the south residual cap can be sorted into definable units. Mapping (by PT) was done in several phases as necessity dictated: First was the general survey (footprints are shown in Fig. 2), then a survey of nearly all the same images was made for some specific forms, most notably topographic moats (Section 3.3.2). A survey of images for shadow measurements, and then for change comparisons were also made. Additional images were remapped for more complete statistics of size distribution of some forms. Fundamentally, the nature of the upper surface, and the types of depressions show the major division of depositional units.

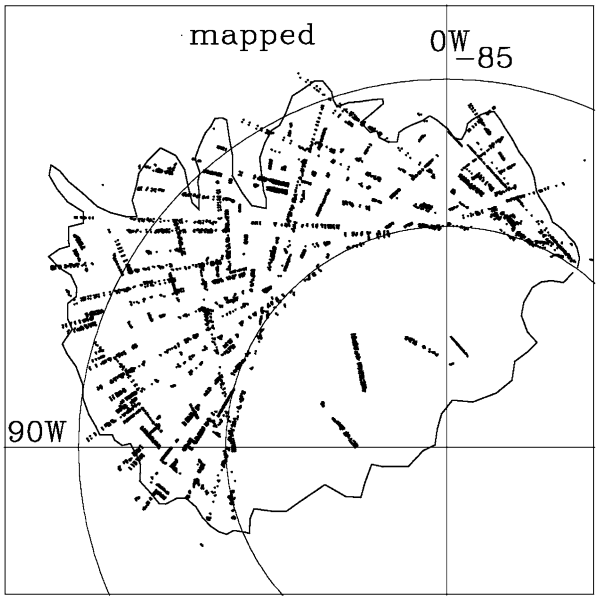

Fig. 2. Footprints of primary mapping data. Approximate average limit of residual cap is outlined. Latitude lines are at 87° and 85° S. The Mars Global surveyor orbital inclination limits most data to latitudes lower than 87° S; some data at higher latitudes were obtained by rolling the spacecraft.

3.2. Unit A

The images show that the residual cap consists of at least two major layered units deposited at different times separated by a period of degradation. The older depositional unit, here termed unit A, is a series of layers, with an upper surface usually marked with polygonal troughs (Figs. 3–6). The unit occurs as erosional remnants of greatly varying extent, usually bounded by moderately steep upper slopes and more gentle lower slopes. In plan these scarps usually define portions of near-circular arcs. These arcs appear to be the remains of expanded depressions. Other depressions occur in the surface of this unit, most notably curled to elongate ones (Figs. 3f, 5a, 5b, 5c, 5i). The polygonal troughs are typically 6–10 m in width, and segments are typically 30–50 m in length. Trough depths cannot be accurately measured, but from the lack of obvious shadows they are less than one m.

The distribution of mesas and other remnants of this unit are mapped in Fig. 4. Unit A was evidently deposited over much the area of what is now the residual cap. While much of this area has had these layers removed, and some remnants are small, other regions have only a small fraction of the surface lost to depressions. No full width (3 km) MOC NA images show unit A without some depressions, but images with less than 10% of the unit A surface area consumed by depressions are common. These areas have patches of undisturbed unit A more than 500 m across. Mesas in some areas (most notably 340°–350° W) follow a linear trend (Albedo patterns associated with these mesa are visible in Viking and Mariner 9 images; see Figs. 25 and 26 of James et al. (1979), and Section 6 below). They run along local topographic crests and steps (less than 50 m relief).

3.2.1. Unit A layer and scarps

We have measured single and double layer thicknesses of parts of unit A using shadow lengths, and of large, higher remnants of unit A using MOLA data from individual tracks overlaid on the images and checked for position matches. Figure 3 shows examples of layer exposures, and Fig. 6 shows the distribution of measured thicknesses. In the measured instances of one and two layers, the individual layers of unit A are ~2 m thick.

However, it is not clear that the stack of layers in all parts of unit A is the same, and in the largest stacks it is not obvious all layers are two m thick. The patterned materials at the foot of the steeper scarps around unit A often give the impression of a large number of thin layers (Figs. 5f, 5g). However, several lines of evidence suggest that in most instances they are debris formed by degradation of thicker layers. In detail, many of the exposures show branching and truncated patterns, which are difficult to associate with any continuous

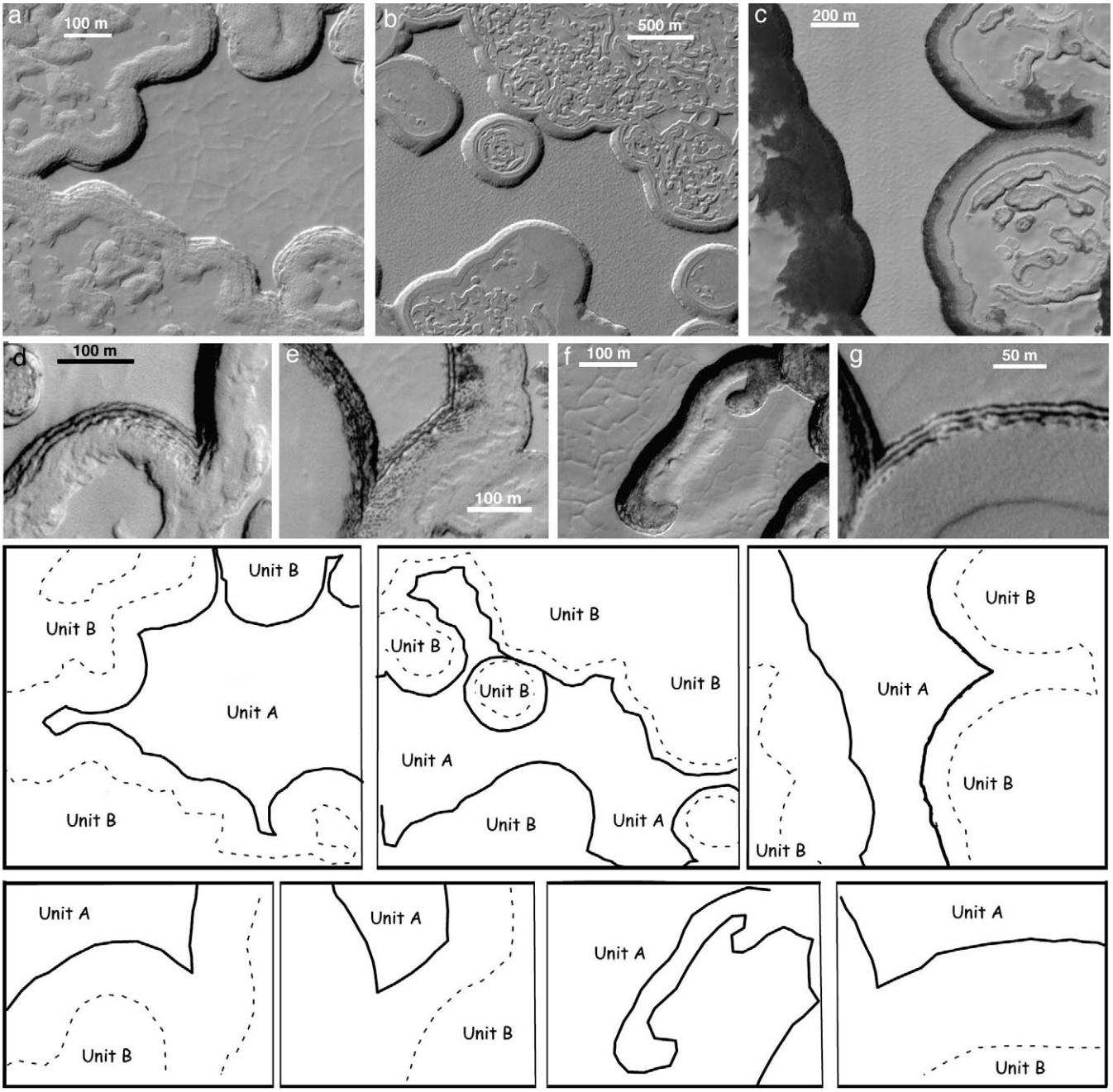

Fig. 3. Surface and margins of unit A. (a) Mesa with scalloped scarps, flanked by moats and unit B. MOC image M09-04089, 86.7° S, 349.2° W, $L_s = 245°$, nazim = 243°. (b) Mesa of unit A flanked by unit B, with large circular depressions in unit A which contain fill of unit B and moats. MOC image M03-06646, 85.4° S, 77.3° W, $L_s = 182°$, nazim = 225°. (c) Late summer image of unit A mesa showing steeper flanks and margin with lower albedo than upper surface of units A and B. MOC image M13-01121, 86.8° S, 344.0° W, $L_s = 320°$, nazim = 246°. (d) Unit A detail showing three exposed layers and moat between units A and B. MOC image M12-01026, 85.9° S, 51.1° W, $L_s = 298°$, nazim = 317°. (e) Mesa of unit A, two layers visible near top, flanked by more complex exposure, probably debris. MOC image E12-00825, 86.5° S, 358.6° W, $L_s = 304°$, nazim = 237°. (f) Elongate depression in unit A with associated collapse feature that retains some of the polygonal troughs typical of the surface of unit A. MOC image E13-00558, 87.0° S, 3.9° W, $L_s = 321°$, nazim = 275°. (g) Layers of unit A and moat between unit A and B. This scarp has at least three layers with relatively dark risers and bright steps. MOC image R11-02744, 86.8° S, 84.0° W, $L_s = 298°$, nazim = 250°. Bottom section delineates prominent sections and boundaries of units A and B.

layers. The exposures of other complex patterns are clearly not consistent with exposure of layers (Figs. 5e, 5f, 5g). For example, in Fig. 5g, the left, more extensive part of the lower, darker material displays twice the number of darker bands as does the narrower exposure to the right. Also, in some areas the upper layer has been degraded apparently under the influence of winds, and has formed material very similar to the lower slope patterns nearby, even though it is clear that only the top layer is involved in the formation of the patterned materials (Fig. 5d). Shadow measurements of the heights of unit A mesas and interiors of large depressions in unit A have heights of 9.3 ± 1.7 m ($n = 68$) (here, and

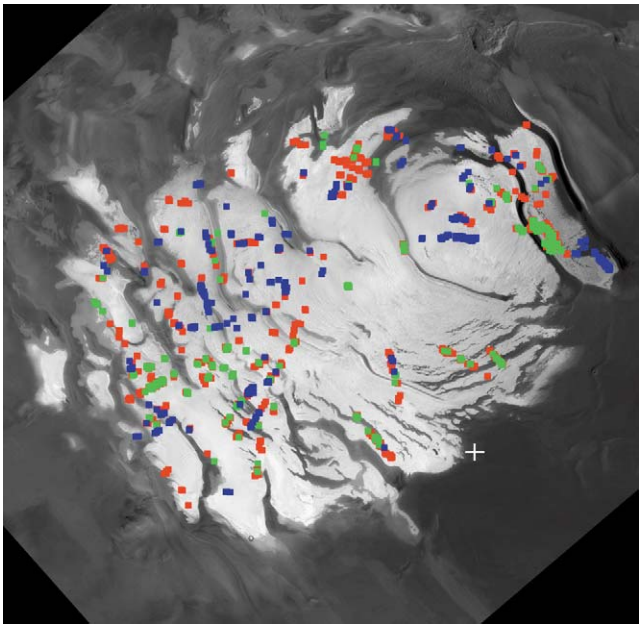

Fig. 4. Distribution of features of unit A. Red points are undistinguished examples of the top of unit A; green points are for large near-circular depressions and remnants in unit A; blue points show curled depressions in unit A. Background mosaic is from MOC WAC images obtained during the E14 cycle. Width of image about 590 km. White cross marks the south pole. Compare to mapped points in Fig. 2.

below, averages are given with one standard deviation, and the number of measurements used). MOLA measurements of mesa remnants of unit A (not all included in shadow measurements) are 10.3 ± 1.7 m ($n = 33$). The coincidence of these measures gives confidence in the shadow technique. The consistency of these height measurements suggests a nearly uniform feature exists over a large area. These heights are relative to the surrounding surface of unit B (see below), which on average would add less than 2 m to the height above the PLD substrate. This thickness of at least 10 and possibly 14 m would suggest at least five ~ 2 m layers. Only slightly thinner layers in the lower portions of some mesas could give 6 or even 7 layers in a stack. The remnants found amenable to MOLA and shadow measurement are scattered widely, ranging in longitudes west from 340° to 77° W, and probably are typical samples of this widespread unit.

Measurement of depths in some of the curl forms in unit A gives consistent values of 8.3 ± 2.0 m ($n = 31$), which are indistinguishable from depths reported by Byrne and Ingersoll (2003b), and are only marginally different from the mesa measurements. However, assigning a number of layers to the curl depth is also difficult due to covering of the lower slopes. Although there is material covering some of the lower slopes of the curls, and their floors are often hummocky in the highest resolution views, the debris at the base of curl interior scarps is less extensive than that around many unit A mesas. There are probably more than 2 layers exposed on average in the curled depressions in unit A. The relationship between the exposed section of unit A in the curls to that in the large circular depressions and mesa edges is not clear as the curls do not occur in conjunction with the mesas whose heights can easily be measured.

The width of the exposures of clearly visible layers (that is, the risers, not the horizontal steps) averages 4.0 ± 2.5 m (57 measurements, 26 images, 1.5 m pixels). If these have an average height of 2 m, the slopes on the individual layer exposures average 27°. This measure, however, is biased toward the more easily measured steps: the wider, shallower exposures. Images viewing along scarps show outcrops of individual layers can be much narrower and smaller than any useful measurement. The slope of the whole scarp is a combination of steep slopes on individual layers, some flat steps at the tops of exposed layers, and often a much more gentle slope on debris at the base of the scarp. The complex materials on the lower portions of the scarps have much lower slopes, as can be inferred from an incremental height of ~ 6 m over ~ 100 m, for a slope of 3.4°. Most of the lower scarp materials extend considerably less than 100 m, so average lower slope values are probably 5°–10°.

This unit may overlie water ice (Titus et al., 2003; Byrne and Ingersoll, 2003a; Bibring et al., 2004), or other materials that are physically or compositionally distinct. What might be called "basement" for these deposits is elusive, partly because of the presence of the younger unit B (see below). Preliminary examination of images for changes over two Mars y in the darker trough walls and some of the complex layers exposed therein have revealed no changes, in contrast to the case for units A and B (Section 5). The lack of visible changes distinguishes the underlying materials from the CO_2 likely composing the residual cap layers.

3.2.2. *Unit A depressions*

Depressions formed by sublimation or other processes give the south residual cap its distinctive appearance. The depressions in unit A can be roughly grouped into approximately circular, curled, and elongate. Circular ones are shown in Figs. 3a, 3b, and 3c. Virtually all of the near-circular depressions show the intricate topography seen in Figs. 3b and 3c, including topographic moats around the scarps in unit A. Other distinctive depressions in unit A include curls, Figs. 5a, 5b, 5c. These depressions have heart-shaped outlines that merge to more elongate forms with curved ends (Fig. 3f). The more convex parts usually have two clearly exposed layers, below which hummocky topography merges into the center of the depression. Many have a ramp from the "open" end to the depression floor. The ramps in Fig. 5b should be compared to the remnant in Fig. 3f, and the asymmetric depression in Fig. 5i. Other curled depressions in unit A show effects of curving fractures (best interpretation). The open ends of the curls preferentially point toward the north (see Section 8; also Byrne and Ingersoll, 2003b).

Sizes of the circular and partial circular depressions are shown in Fig. 7a. The distribution of sizes for complete circular depressions and sizes inferred from incomplete remnants are indistinguishable. The partial ones (Figs. 3a

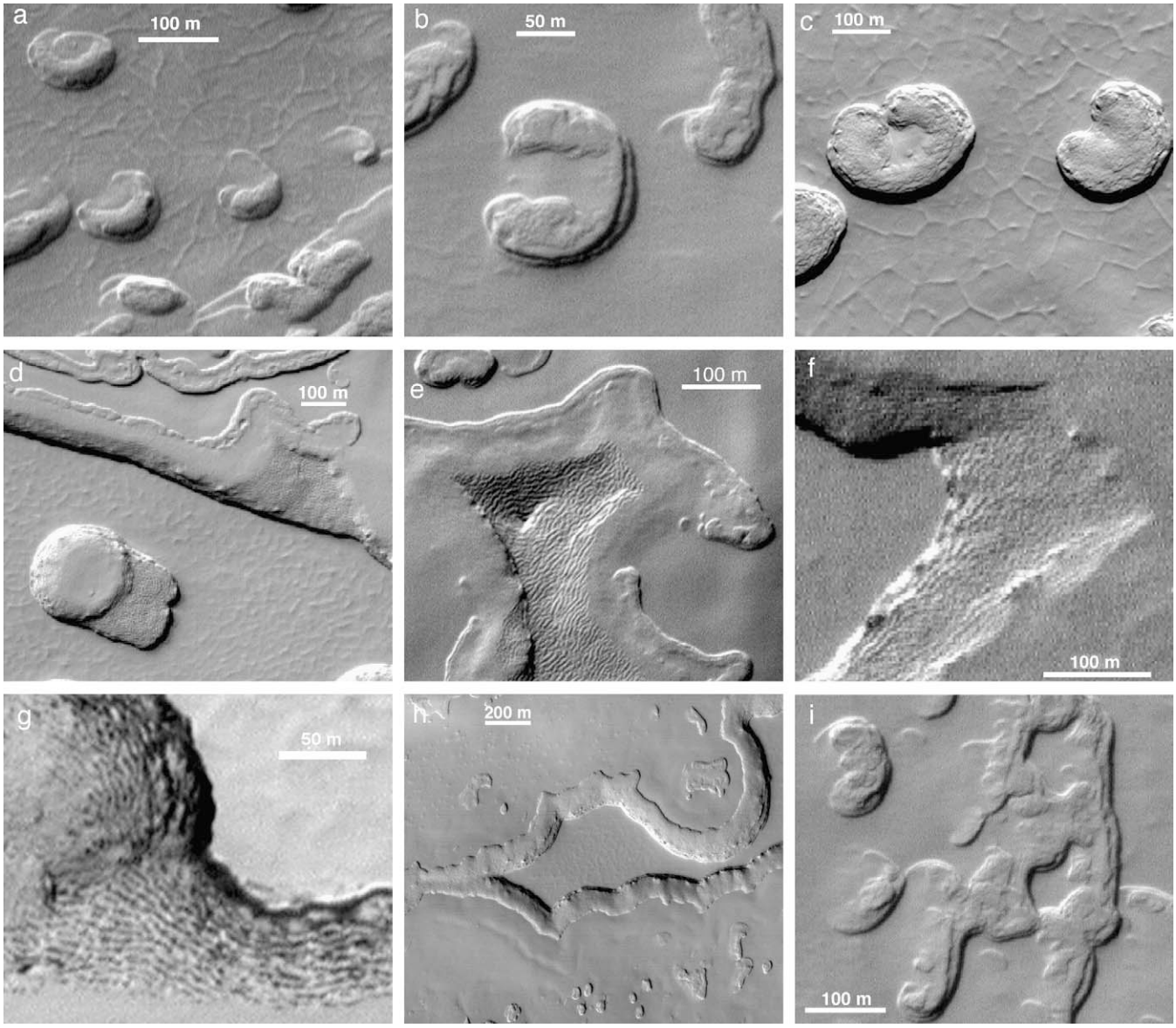

Fig. 5. Modification of unit A. (a) Series of depressions with what may be fracture margins, possibly showing several stages of development of depressions, going from the right middle to left middle, then to the upper left. MOC image M07-02129, 87.0° S, 75.9° W, $L_s = 204°$, nazim = 251°. (b) A curl depression, showing the central ramp-like feature; compare to Fig. 3f. MOC image M08-07868, 86.3° S, 49.6° W, $L_s = 234°$, nazim = 234°. (c) Curl depressions in unit A. Note the suggestions of former ramps from the cusp region. MOC image E10-00804, 87.0° S, 6.1° W, $L_s = 266°$, nazim = 275°. (d) Unit A depression elongated by wind, and margin of mesa. Elongated portion of depression is only one layer down and is floored by patterned material similar to that surrounding the mesa at top of the image. MOC image M08-05817, 86.7° S, 348.2° W, $L_s = 230°$, nazim = 296°. (e) Remnant of unit A nearly completely collapsed, surrounded by moat and unit B. The patterned material is similar to that seen around mesa scarps, but here the extensive pattern cannot be distorted layers. MOC image M09-01595, 86.5° S, 349.2° W, $L_s = 239°$, nazim = 236°. (f) Mesa of unit A and debris. Debris might give impression of many layers, but in detail does not represent continuous layer exposures. MOC image M08-04356, 87.1° S, 340.7° W, $L_s = 227°$, nazim = 266°. (g) Debris around mesa of unit A. MOC image E12-00825, 86.5° S, 358.4° W, $L_s = 304°$, nazim = 237°. (h) Mesa of unit A with moat separating it from unit B, which embays circular depression remnants in unit A. MOC image M09-03306, 86.2° S, 70.4° W, $L_s = 243°$, nazim = 312°. (i) Elongate and curled depressions, possibly defined by fractures. MOC image M08-07868, 86.3° S, 49.0° W, $L_s = 266°$, nazim = 233°.

and 3c) do not indicate a different generation, simply development in higher spatial densities such that development interfered with complete outlines. We have tabulated the elevation, slope, and slope azimuths from the MOLA gridded data for the mapped features, and sought distinguishing conditions of occurrence. Few, if any, compelling ones exist. The large circular depressions in unit A have a moderate preference for low slopes (most occur on slopes $< 0.3°$) compared to the average slope in the residual cap ($\sim 0.5°$), and the curls occur on slopes with a distribution similar to that on the overall residual cap.

3.3. Unit B

Surrounding the remnants of unit A are thinner, mostly smooth-surfaced deposits, here termed unit B, occurring in

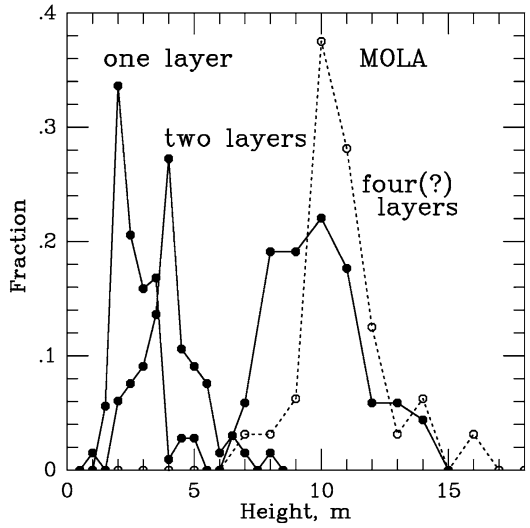

Fig. 6. Thicknesses of some layers exposed in unit A. Heavy solid lines with filled symbols show shadow measurement results. Those labeled one and two layers are reliably seen as distinct layers. The data centered around 10 M are for exposures of unit A relative to surroundings, such as those in Figs. 3a, 3b, 3c. MOLA data (dashed line) were used to check the average results of the shadow measurements for the mesas and indicate that the shadow measurements are reliable.

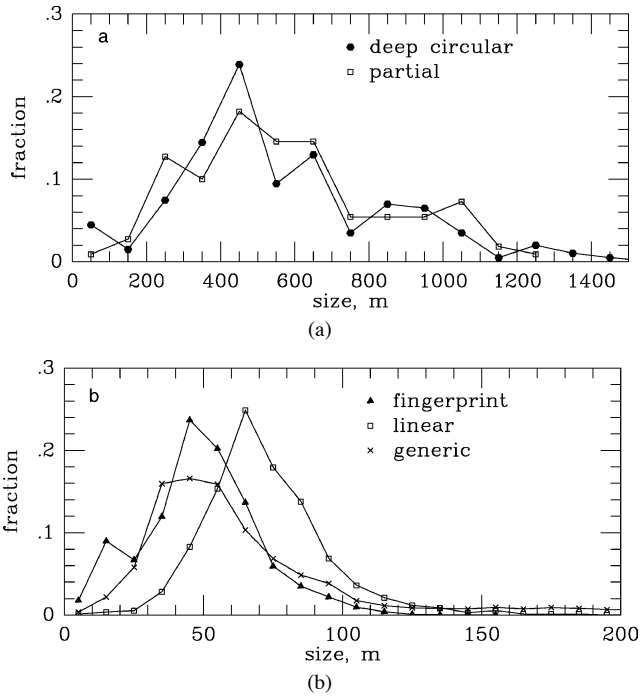

Fig. 7. Size distribution of selected types of depressions in units A and B. $n =$ designations are number of measurements. (a) Diameters of roughly circular depressions included in data shown in Fig. 3b, and of partial remains of circular depressions (Fig. 3c). (b) Widths and diameters of depressions in unit B. These are data acquired while mapping samples in each image, thus are not complete descriptions of the size ranges. They do accurately reflect that most depressions in unit B are less than 100 m across, and linear depressions (Fig. 8b) and fingerprint (Fig. 8d) ones have strongly preferred sizes.

one to three layers (Fig. 8). These materials are usually distinguished from unit A by their smoother surfaces, thinner layers, different erosional style and types of depressions, and by unconformable contact with parts of unit A. Occurrences of unit B features are mapped in Fig. 9.

3.3.1. Unit B layers

Layers in unit B are clearly thinner than the well-resolved ones in unit A when seen in the same image. They are sufficiently thin that reliable height measurement using shadows is not possible in many views. Good shadow measurements require 1.5 m pixels, incidence angles over 65°, and forms that cast distinctive shadow shapes so that it is clear shadows are measured and not shading or even moat edges. Measurement from MOLA data is essentially ruled out by the laser footprint size ($\sim$ 150 m), spacing ($\sim$ 300 m), and by the size and spacing of depressions in unit B. Nonetheless, we have found a modest number of good shadows to measure the thicknesses of some single and double layer sections of unit B. The single layers average 1.1 ± 0.4 m ($n = 55$), double ones 2.4 ± 0.5 m ($n = 12$). The most important result of these measures of $\sim$ 1 m/layers is that layer B materials are further distinguished from the upper, well-measured, layers of unit A. One of the perplexing aspects of the photogeologic and stratigraphic nature of the south residual cap is that the later unit B post-dates and unconformably overlies unit A debris, yet apparently was not deposited or did not persist on top of most unit A outcrops. This situation is indicated by the survival of the polygonal surface on unit A, its more ragged backwasting (scarp retreat) pattern, and the difference in thickness of the top layers from those in nearby unit B.

3.3.2. Unit B depressions

Unit B displays an even greater variety of depressions than does unit A, even though it is younger. It has some nearly circular depressions, large numbers of highly irregular depressions (Fig. 8), heart-shaped ones analogous to the curls in unit A, a wide variety of long, sinuous depressions, linear depressions termed fingerprint terrain, and a variety of moat forms between scarps of different heights.

The central part of the mapped portion of the residual cap is dominated by a two-layer section that is cut largely by linear, roughly parallel depressions informally termed fingerprint terrain (Thomas et al., 2000) (Fig. 8d). These depressions show asymmetric cross sections, with a steep side, exposing layers, a flat or v-shaped bottom, a much more gently-sloping opposite face, and usually an intervening relatively flat area between depressions (Fig. 8d). This surface presents interpretive problems, but in most areas it appears to be more easily mapped as unit B than A. This designation is supported in these areas by the smoother surface and the distinct position of nearby obvious outliers of unit A. However, there are some faint polygonal marks in some areas with fingerprint depressions, and the depth of these depressions (3.5 ± 1.3 m, $n = 166$) suggests layers between 1 and 2 m thick. The fingerprint depressions have remarkable consistency in orientation and sizes over more than 200 km

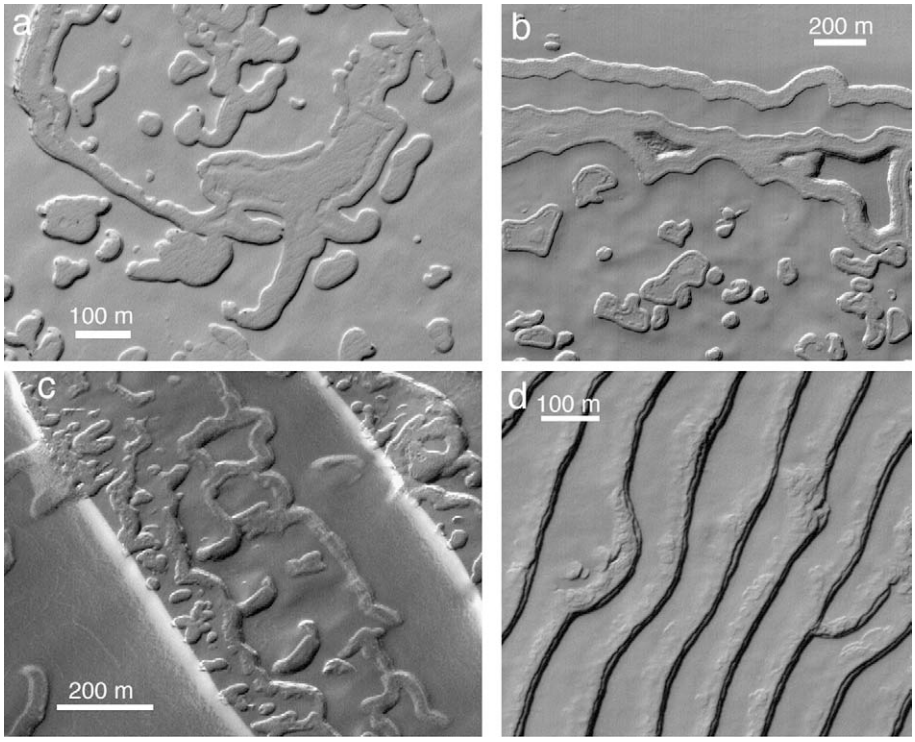

Fig. 8. Unit B examples. (a) Typical surface of unit B with different shapes of depressions and hints of narrow moats in some depressions. MOC image E11-01025, 85.1° S, 30.0° W, $L_s = 284°$, nazim = 306°. (b) Linear depressions in unit B. These commonly form parallel to edges of the unit on troughs, but occur in other areas, often with substantial sinuosity. MOC image E09-00269, 87.0° S, 86.8° W, $L_s = 246°$, nazim = 255°. (c) Complex layer overlap in unit B. MOC image M04-03877, 84.7° S, 44.5° W, $L_s = 196°$, nazim = 213°. (d) Fingerprint terrain. MOC image M08-07868, 86.2° S, 50.5° W, $L_s = 234°$, nazim = 233°. Note the tuning-fork junction, with apparent two-layer exposures in the steeper walls on the right.

distance. Unlike the simple curl depressions, their orientations change with longitude and present a largely coherent pattern (Section 8.3), albeit with strong local variations associated with changes in topographic slope.

Other depressions in unit B are long, sinuous ones, commonly found near the break in slope of troughs in the polar layered deposits (Fig. 8b). These grade into a variety of curling depressions. Apart from their less organized patterns, these are distinguished from the fingerprint depressions by their short-dimension symmetry, and usually by their formation in thinner materials. These widths are plotted in Fig. 7b as "linear" depressions. These width tabulations (from the mapping survey, and not a complete sample of all forms in an area) show why many of the forms merge in casual (or even close) inspection: there is a preferred family of widths. The linear depressions are about 45% wider than the fingerprints (both peak occurrences and averages).

Many depressions within unit B (Figs. 10c, 10e), display topographic moats, which provide further information on the history of unit B. All moats in the south polar residual cap either are within exposures of unit B or are between units A and B (Figs. 10a, 10b). All the moats are placed between scarps of different heights. Material making moats in depressions is always thinner than the enclosing materials (Fig. 10c). A striking feature of many areas of unit B is the additional set of smaller moats within larger moats, such as

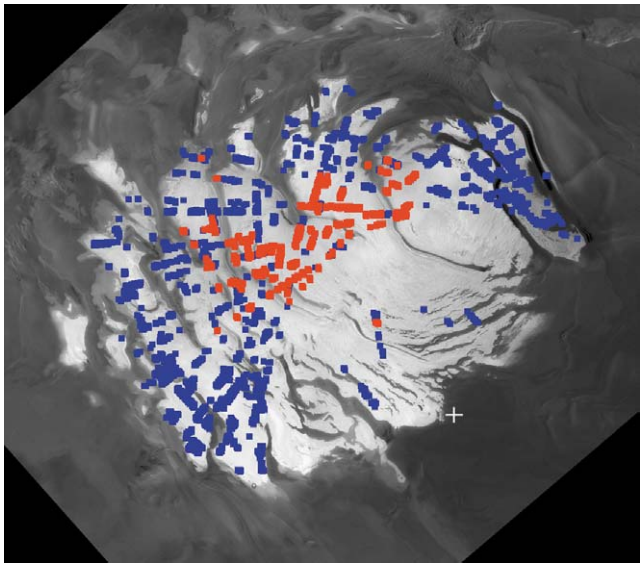

Fig. 9. Unit B feature locations. Red points show fingerprint terrain locales; blue marks other typical unit B depressions. Cross shows south pole, 0° longitude is at top, 90° W is at the left. Image width about 590 km.

easily seen in Fig. 10e and more subtly displayed in Fig. 10c. Moats surround nearly all unit A scarps; examples appear in Figs. 3a–3e, and 3g. They are also shown in Figs. 5d and 5h, and Figs. 10b, 10d. The moat in Fig. 10b is a large moat

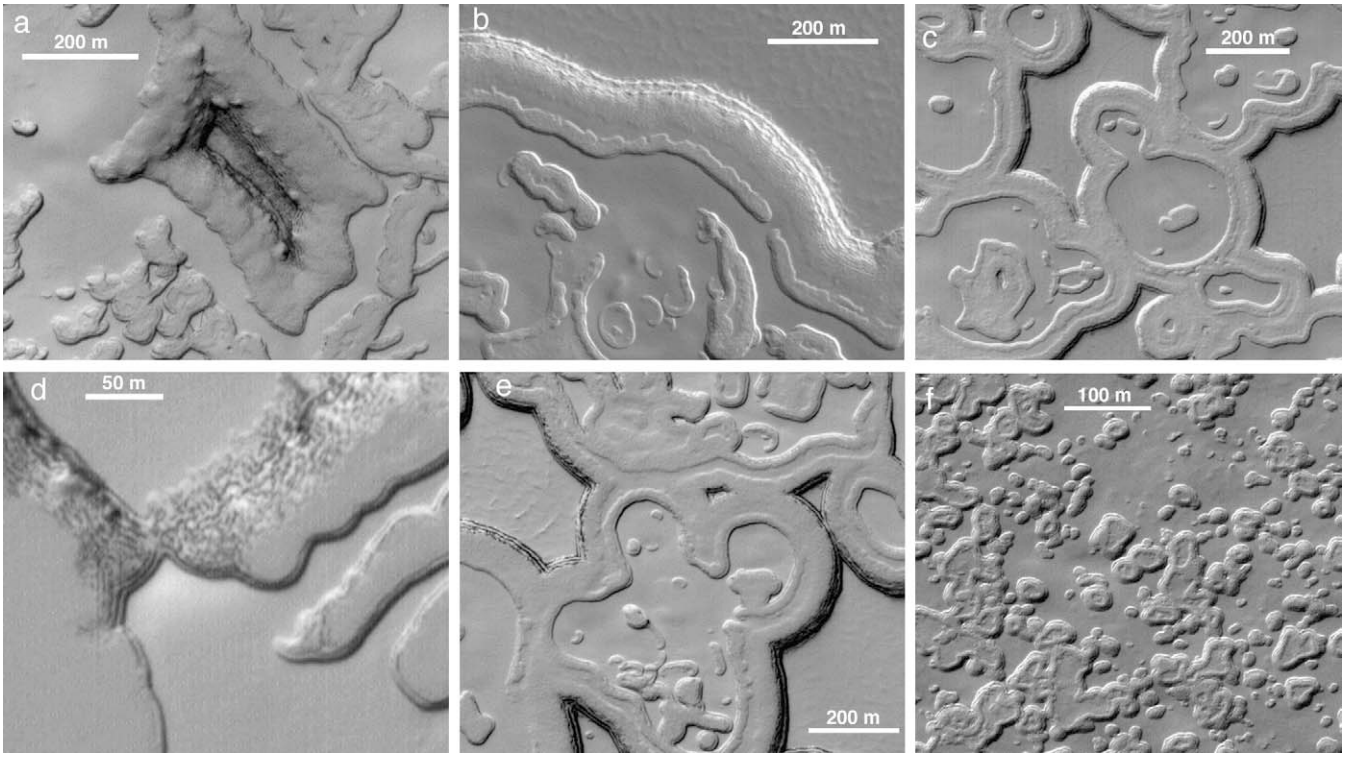

Fig. 10. Moats in unit B and relation of unit B to unit A. (a) Moats in unit B surrounding highly degraded remnant of unit A. MOC image E12-01117, 86.4° S, 67.0° W, $L_s = 305°$, nazim = 308°. (b) Erosion of unit B resulted in a double moat surrounding unit A mesa. MOC image R07-01203, 86.9° S, 343.6° W, $L_s = 223°$, nazim = 231°. (c) Three layers of unit B with two generations of moat formation. Most prominent moats are flanked by narrower moats. Medial material is thinnest deposit; next in thickness is depression fill that defines the most prominent moats, and thickest is the material at right, top, and bottom defining the outside of the most prominent moats. MOC image E09-00269, 87.0° S, 85.2° W, $L_s = 245°$, nazim = 255°. (d) Unit B unconformably overlying debris from degradation of unit A. There appear to be three unit B layers here. MOC image R12-00656, 84.7° S, 52.8° W, $L_s = 309°$. (e) Double moats flanked by unit A and B. MOC image R11-02744, 86.8° S, 83.8° W, $L_s = 298°$, nazim = 251°. (f) Small depressions and larger ones with moats occur in a variety of irregular shapes. Material filling depressions forming the interior wall of moats is thinner than outer materials. MOC image M08-02086, 86.0° S, 87.3° W, $L_s = 221°$, nazim = 230°.

between unit A scarp and unit B, with a smaller one in the unit B material. This latter moat is a type that forms on convex exposures of unit B, but is similar in dimensions to the secondary ones within depressions of only unit B materials (Figs. 10c, 10e). Moats are also found in highly irregular depressions in unit B, but maintain the striking constancy of widths. Moats between units A and B can form around subdued remnants of unit A (Fig. 10a) as well as around steep scarps.

Moats in unit B have a bimodal size distribution (Fig. 11), and there is a virtual absence of moats within depressions less than 40 m diameter. The bimodal distribution applies to those in nearly circular depressions as well as those in highly irregular depressions. Moats between unit A and B are nearly the same size as the larger ones in unit B. In Section 8 the geometry of the moats is used in reconstruction of deposition and erosional events of unit B.

This bimodality of moat widths, the occurrence of narrow moats within larger ones (Fig. 10e), and the observation that moated material inside depressions is always thinner than the surrounding materials is most easily explained by deposition of a layer after erosion of moats to an average width of about 50 m, followed by more backwasting of all layers.

3.3.3. *Distinctiveness of residual cap layers*

Both units A and B differ from the seasonal CO_2 cap. Unit A layers, and some in unit B, are thicker than the ~ 1 m deep annual cap (Kieffer et al., 2000; Smith et al., 2001). Both units have higher albedos than the annual cap, which also has a wide variety of optical properties (Kieffer et al., 2000). They lack the odd markings such as "spiders" or the many varieties of plume-shaped (and generally lower albedo) streaks found in the annual cap (Kieffer, 2003). The greatest distinction of the residual cap materials from the annual cap is of course their survival of the summer season.

4. Stratigraphy

We summarize here the stratigraphy of the south polar residual cap from a photogeologic standpoint.

First, the layers of unit A are the older deposits. This relationship is shown by the embaying of unit A by unit B (Figs. 3a, 3c, 5h), unconformable deposition of unit B on debris from erosion of unit A scarps (Fig. 10d), and the widespread occurrence of overlap and moats such as that in Fig. 10a, which is little different from the B unit over-

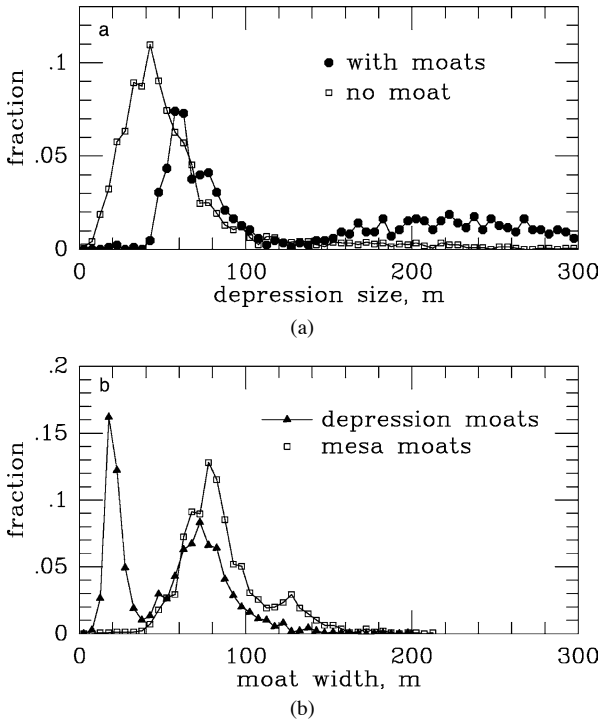

Fig. 11. Moat and depression sizes. Data taken from images specifically remapped for moat statistics. (a) Depressions in unit B, classed by whether a moat is present. Depressions in these images smaller than 40 m had essentially no moats. See Figs. 10f and 13a for examples where large depressions have moats, smaller ones do not. Note also the sampling of more irregularly shaped depressions yields a wider size distribution than in Fig. 7b. (b) Widths of moats in unit B and between unit B and A (mesa moats). The bimodality of the moats may be seen in individual images such as Figs. 10c, 10e.

lap of debris shown in Fig. 10d. The latter example simply has a still-standing scarp of all the layers in the stack; the remnant in Fig. 10a has lost organized remains of the upper layers of unit A. Fig. 4 shows that unit A was widespread over the present area of the residual cap, with a considerable variation in its preservation: compare Fig. 10a with Figs. 3 and 5.

Second, unit A was substantially eroded before unit B was deposited. See all the above examples: unit B is in large circular depressions in unit A, and covers remnants of these large circular depressions (Figs. 3b and 3c). In Section 8 below, we investigate actual timescales for change in the residual cap deposits.

Third, at least one layer of unit B was deposited. We note here, and discuss further below in Section 8, the remarkable indication that unit B is not retained on top of much of unit A. It was deposited up to unit A scarps and within unit A depressions, but if it was deposited on the upper surface of unit A it has been subsequently lost.

Fourth, unit B started to erode, by backwasting. This process is shown by the depressions that opened in unit B; unit A may have been backwasting as well. Details of subsequent events in unit B are shown by the moat geometry and size distribution of features. Here we simply note the steps.

Fifth, erosion was interrupted and another layer deposited over the area of unit B. This layer forms the bulk of deposits inside depression moats such as in Figs. 10c, 10e.

Sixth, backwasting resumed, with the immediate effect that moats formed in areas with offset top surface heights, such as in depressions that have received fill.

Seventh, another depositional episode followed after moats had opened up an average of 50 m widths (difference in peaks of most size distribution, Fig. 11b).

Eight, backwasting resumed, forming double moats in many of the older moats. Backwasting continues.

We note that the layers of both units each imply some change in conditions, and as a group, they may indicate a change from the underlying polar layered deposits. The development of the layers and depressions is discussed further in Section 8.

5. Recent changes observed in the residual cap

Scarp retreat of order 3 m during one martian year has previously been documented in MOC images in a few areas of the south residual cap (Malin et al., 2001). The images examined showed loss of septa between depressions, expansion of depressions, and change of shape of some features. As most of the images were ~ 3 m/pixel, the one-year change of 3 m was detected, but not accurately measured or fully mapped.

5.1. Two-year changes measured in MOC high-resolution images

A second year of changes is documented in the relay orbits (R images) obtained in late 2003. Examples of two-year changes in units A and B are given in Figs. 12 and 13. We have mapped hundreds of additional one and two-year changes of several types of features in the residual cap. Although changes are visible in images of several m/pixel, the mapping has concentrated on those with pixel scales of 1.5 to 2.2 m. The results are summarized in Table 1 and Fig. 14. M orbit measurements were done between $L_s = 220°$ and $L_s = 275°$, with exceptions at $L_s = 186°$, 293°, and 303°. R orbit measurements were done within 10° of L_s of M orbit observations, with the exceptions of the comparisons to the late season M data done much earlier in the summer season. Nearly all these observations are from times when the seasonal cap was partially present, thus the changes between most of our M and R images took place in the later parts of the summer covered by the M and E images, not in the summer covered by the R images. Exclusion of the late summer (M; $L_s > 290°$) data does not give any change in the average rate for unit A, and only a 3% difference for unit B.

The first result is that changes continued for a second year, at roughly the same rate as observed by Malin et al. (2001).

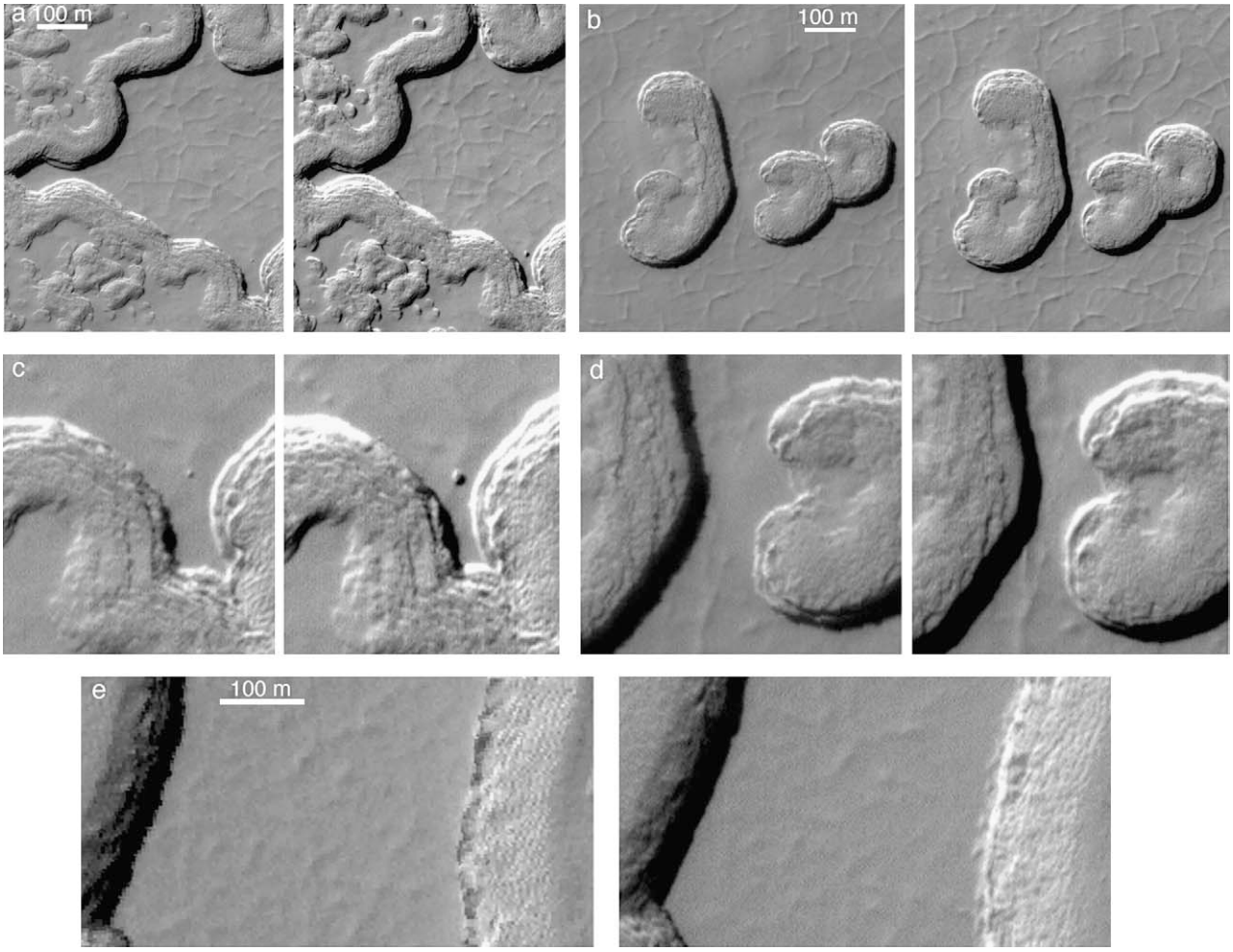

Fig. 12. Changes in unit A over 2 Mars years. (a) MOC images M09-04089, $L_s = 245°$ and R08-0987, $L_s = 239°$, 86.7° S, 4.7° W. (b) MOC images M09-00609, $L_s = 236°$ and R08-01050, $L_s = 241°$, 87.0° S, 6.5° W. (c) Detail of A. (d) Detail of b. (e) Detail of MOC images M10-00093, $L_s = 254°$ and R08-00040, $L_s = 232°$, 86.8° S, 344.8° W.

The second finding is that unit A is eroding more rapidly than unit B. One-sigma error bars slightly overlap (Table 1), but the distribution of the measurements makes clear that unit A behaves differently from unit B (Fig. 14). Note that the rates in the table are for two years of changes of diameters or widths, thus, the rate of backwasting of a scarp face is 1/4 the value given in the 2 y change column of the table. Unit A scarps retreat at an average of 3.6 m/Mars y, unit B scarps retreat at 2.2 m/Mars y. There are few measures of large circular depressions in unit A partly because of limited coverage as of this writing, but also partly because the fairly ragged nature of the upper slopes of many unit A scarps makes comparison between images taken under slightly different lighting conditions somewhat difficult. The changes in curls are indistinguishable from those in the rest of unit A, measured in very different-looking forms. The fingerprint terrain and the various kinds of moats in unit B change at rates indistinguishable from changes in average depressions and septa between depressions. It is reassuring that the rate of expansion of moats between units A and B is intermediate between the rates of A and B retreat.

The third finding is revealed by the above statistics: all types of moats are expanding. The moats cannot be equilibrium forms retreating with scarps; this was a concern in early viewing of the images that showed remarkable consistency of moat widths, and was suggested as a possible process by Byrne and Ingersoll (2003b). We emphasize that all types of moats, multi-generational within circular depressions, single small ones in unit B, and those between units A and B, are expanding. This observation is important below in the discussion of mechanisms and timescales.

A fourth, and equally important result, is one derived from the cumulative observations of all the south polar images and is entirely in concert with the measurements: all the upper surface topography of the residual cap is erosional. There are no indications of any summer redeposition of CO_2 within the cap: the edges of scarps remain crisp, even ragged, the polygonal troughs (depths of much less than a m) are retained year to year, albedo features remain constant in similar seasons, and other very small scale topography (fractures, layer edges, and very small pits) remain or ex-

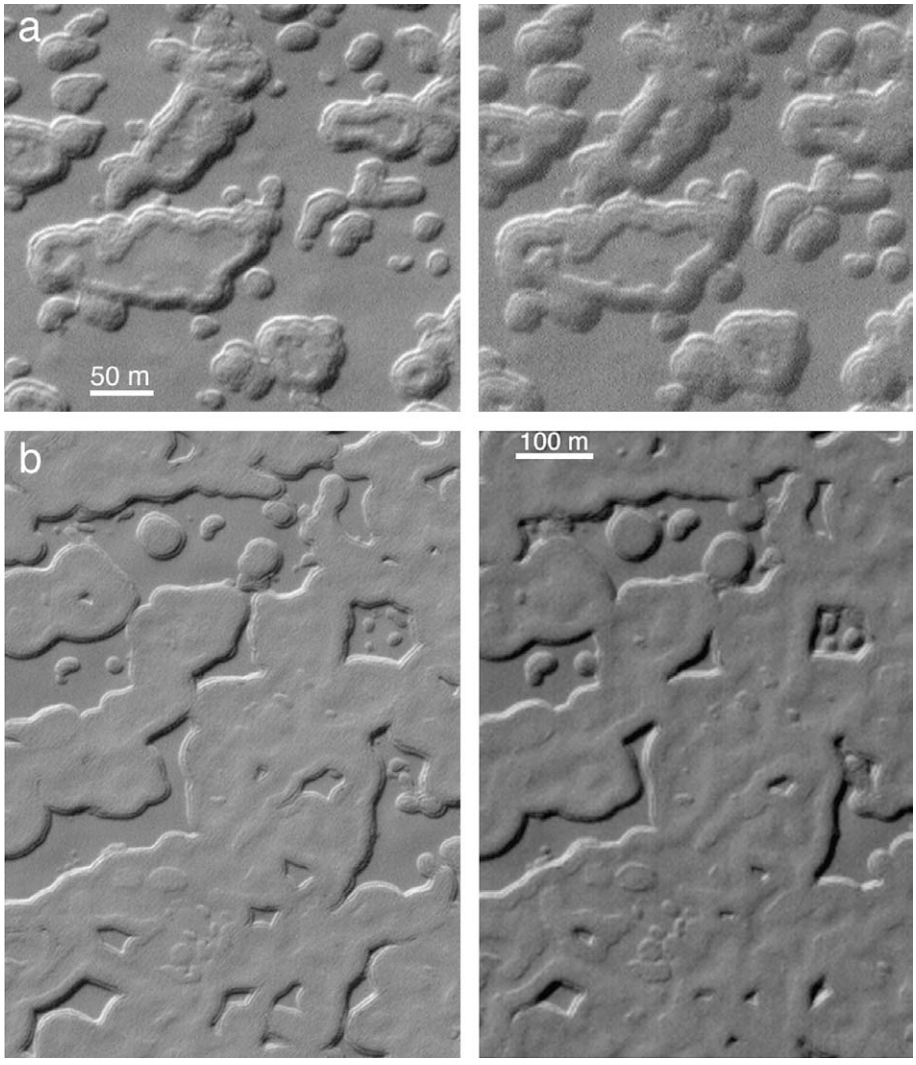

Fig. 13. Changes in unit B over 2 Mars y. (a) MOC images M08-02086, $L_s = 221°$, left, R06-01503, $L_s = 209°$, right, 86.0° S, 87.2° W. (b) MOC images M09-01686, $L_s = 239°$ and R07-02203, $L_s = 231°$, 86.8° S, 98.9° W.

Table 1
Rates of scarp retreat in south residual cap

Type	Change, m[a] 1 y	Change, m[a] 2 y	Size m	Timescale Mars y	# ch obs	# size obs
Unit A	6.8 ± 2.6	14.2 ± 3.2 (2.0)[b]			109	
Unit B	4.6 ± 2.4	8.6 ± 2.7 (2.1)			317	
Large circular[c]		15.0 ± 3.4 (4.1)	575 ± 260	77	8	310
Curl[c]		14.3 ± 3.2 (1.7)	200.4 ± 59.5	28	37	466
Generic B		[8.6][d]	45.0 ± 31.3	11		5821
Linear B		[8.6]	72.1 ± 23.7	17		1502
Fingerprint		7.0 ± 2.6 (2.1)	48.7 ± 20.8	14	33	2639
Moat (B large)		9.1 ± 3.8 (2.1)	75.8 ± 19.9	17	38	1150
Moat (B small)		6.4 ± 2.2 (1.5)	20.7 ± 5.5	7	68	740
Moat (B unconfined)		8.1 ± 3.8 (2.3)	31.8 ± 26.7	8	63	63
Moat (A–B)		12.0 ± 3.9 (2.2)	86.2 ± 24.9	14	52	1384

Note. Uncertainties in rates and sizes are one standard deviation of measurements. # ch obs is number of observations of change, # size obs is number of size measurements mapped.

[a] Sizes and changes were determined by interactive digital measurement of raw MOC images. The change is the difference in diameter of a depression or of septa between depressions for one or two Mars years. 1-year changes measured in 18 image pairs; 2-year changes measured in 27 image pairs.

[b] Parenthetical values for 2-year changes are the mean pixel scales of images used.

[c] Large circular and Curls are depressions in unit A; the remaining listed forms involve unit B.

[d] Values for average unit B used.

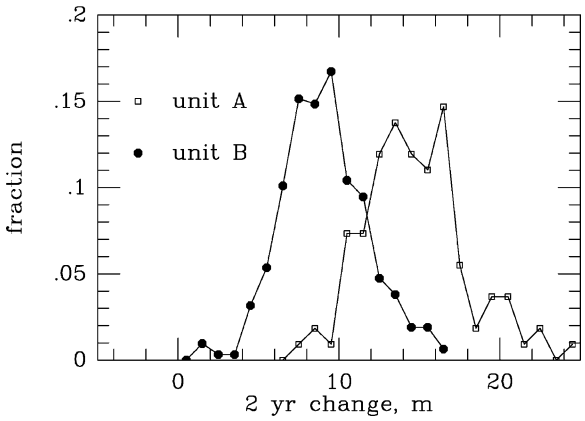

Fig. 14. Change over 2 Mars years in units A and B. Data are summarized in the first two lines of Table 1. Quantity is the change in diameter of depressions or width of septa. Single year retreat of a scarp face is thus 1/4 these values. Unit A is backwasting faster than unit B.

pand. Any summer sequestering of CO_2 in the area of the cap is minimal.

The polygonal troughs in the top of unit A do not show discernable changes over the two years. These are, in fact, good reference marks for documenting changes in depressions, as the depression walls expand through, or clearly nearer to, some of the troughs.

The debris at the foot of scarps of unit A and what we interpret as collapse material have been checked for changes in a few locales with inconclusive results. Slightly different lighting and the complex forms at the few m scale make this a difficult measurement.

Attempts to measure changes in the north residual cap morphology have not been successful. The image coverage is less dense, and the few repeat candidates do not have distinctive shapes to match (see top of Fig. 1a to appreciate matching this topography under slightly varying lighting).

5.2. *Implications of the observed retreat rates*

Application of the observed erosion rates to the history of the south residual cap is complicated by the obvious fact that conditions have changed. Thus, a linear application of the present rate of scarp retreat to all of the present erosional cycle may not be correct. Application to all previous erosional cycles is even more uncertain. However, the interpretation that there are discrete erosional/depositional episodes suggests there might be some processes that can occur at similar rates once turned on. The initiation of many of the depressions appears to involve collapse (Thomas et al., 2000; Byrne and Ingersoll, 2003b), Fig. 3f, so there was an unknown time between initiation of depressions and the start of backwasting. Because the erosion appears to have been in local, expanding centers, the formation time of the large circular depressions may be the best approximation of the time to erode unit A: several tens of Mars y to well over 100 Mars y (Table 1). The timescale for the curls is somewhat shorter, and is much lower than previously modeled (Byrne and Ingersoll, 2003b) because the measured rates of scarp retreat (3.6 m/Mars y) are much higher than their assumed rates (0.5–2.5 m/Mars y). The actual timescale for expansion of unit A curl walls may be even shorter than calculated because the applicable distance may not be the full diameter, but rather the diameter minus a ramp (collapse?) width (see Figs. 5b, 5c).

The length of the time between the initial halt in erosion of unit A and the start of erosion of unit B is indeterminate. Neither unit has impact craters, so this technique is not available for stratigraphic information. Most depressions in unit B could have formed in 10–20 Mars y, although the largest depressions (Fig. 10c), which contain the population of large ($\sim$ 75 m) moats, should have taken several Mars decades to form.

We may summarize the combination of rates and stratigraphic interpretations:

- Formation of unit A: unknown time before present, more than 150 Mars years ago.
- Erosion of unit A before unit B: $\sim$ 100 Mars y (erosion times of largest A depression less erosion time of largest B depressions).
- Unit B largest depression formation: $\sim$ 45 Mars y.
- Fingerprint formation: 14 Mars y.
- Moats between unit A and B: 14 Mars y.
- Unit B large moat formation, 1st stage: $\sim$ 10 Mars y.
- Unit B moat formation, 2nd stage: $\sim$ 7 Mars y.

The time scales reported in Table 1 can be combined to give a possible depositional and erosional history as shown in Fig. 15. The largest depressions in units A and B are used to estimate their possible depositional ages. The time to deposit layers is assumed to be short (see Section 10). The moat dimensions combined with the rates of expansion give the timing of deposition of additional layers on unit B.

6. Changes in the residual cap since Mariner 9 observations

Mariner 9's narrow angle camera (B frames) obtained southern summer images of the south residual cap at 90+ m/pixel (Murray et al., 1972). These images were higher resolution than those obtained by Viking in the late 1970's. Comparison of the Mariner 9 and Viking data showed less area of high albedo in the Mariner 9 images than in the Viking (James et al., 1979, 1992). Mesas of unit A and their included large depressions, and possibly some features in unit B are visible in Mariner 9 images taken in 1972 (Figs. 16, 17). Although the 95–100 m pixel scales of the Mariner images prevent accurate measurement of the changes, the comparisons show important characteristics. From the scarp retreat rates in Table 1, the 15 Mars y between 1972 and 2001 would yield between 50 and 60 m of scarp retreat. With identical lighting on a smooth,

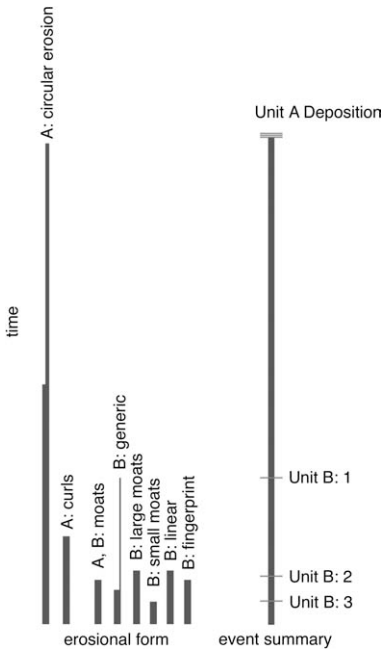

Fig. 15. Scheme for history of deposition and erosion in the south polar residual cap. Vertical bars represent erosion, horizontal bars are depositional periods. The bars on the left are strict tabulations of relative times from Table 1. The thicker parts of the A: circular erosion and B: generic are the times to erode the mean size depressions; the thinner, longer bar accounts for the largest depressions. The highest bar would be about 150 Mars years. The right side shows an approximate summary of implications of the various rate measurements. The numbered B's are times of individual layers in unit B. The depositional times for unit A layers are also assumed to be relatively short. The entire time could be greater due to cessation of erosion or changed rates.

high contrast boundary, such a difference might be easily measured, as coordinates of smooth, high contrast objects can be measured to ~0.1 pixels. However, the somewhat ragged boundaries of the depressions, changing lighting, and changing albedo patterns, make quantitative comparisons of depression sizes between Mariner 9 and MOC good only to about the 100 m level. While we cannot derive a better average rate of scarp retreat during this interval, it is clear that the large depressions are not very different at the 100 m scale, thus backwasting since 1972 could not have averaged multiple times the currently observed rates. Some of the images suggest the breaching of thin septa of unit A in the interim (Fig. 17). This interpretation suggests that there has been more backwasting in the interval than that observed in the last two years.

At the 100 m to few-km scale the south residual cap was more variegated than observed 2 Mars y later by Viking (James et al., 1979) and compared to the three seasons observed by MOC (Figs. 16, 17). James et al. (1992) suggested that additional deposition had occurred between the Mariner 9 and Viking observations. The timescales of formation of many of the unit B moats and depressions are less than the 16 Mars y since Mariner 9 (from 2003). The difference between the MOC and Mariner 9 views shown in Fig. 17b certainly suggests deposition of material in the intervening time that remains at the end of the summer. However, Fig. 17a suggests the situation is not simple, and may have involved spatial variations in the thickness of the unit B layer. The dark area, probably wind enhanced, appears to be an exposure of the distinct material upon which unit B (and A) rest. It is uncovered both at Mariner and MOC epochs. The interiors of the small curling depressions to the right of the dark area in Fig. 17a, and darker margins, is probably the thin, last portion of unit B. However, it either has been removed more rapidly from the dark area, or was not deposited on it.

In summary, the Mariner 9 images are consistent with the current rates of backwasting of unit A, and suggest deposition of a unit B layer shortly after 1972.

7. Rates of change and the CO_2 budget

The net mass loss of CO_2 from the south residual cap was previously calculated (Malin et al., 2001) on the basis of an average 3 m scarp retreat per Mars year. The active perimeter was estimated from boundary analysis of mosaiced images to be $\sim 2 \times 10^9$ m over the present residual cap. These parameters yield a volume loss, which combined with an estimated density of 1.5 g/cm^3, gives a sublimation of 2–4 $\times 10^{16}$ g, or ~0.1% to 0.2% of the atmospheric mass per Mars year. We take a different approach here to estimate the release of CO_2 on a longer timescale by applying the current scarp retreat rates, as the estimation of the active perimeter poses considerable challenges. The removal of unit A (~10 m thick), over ~50% of the 87,000 km^2 of the south residual cap, represents a volume change of $\sim 4.4 \times 10^{17}$ cm^3. A deposit density of 1.5 g/cm^3, appropriate for CO_2 ice, yields a mass of 6.5×10^{17} g, or about 3% of the atmospheric mass (2.2×10^{19} g; Zurek et al., 1992). If removed in the average time scale calculated (77 Mars y), this quantity would indicate a removal rate of ~0.04% atmospheric mass per Mars year. Such a change would not have been detected by the Viking pressure measurements and would be difficult to detect even from measurements obtained over many more years (Paige and Wood, 1992). Smith et al. (2001) estimate a somewhat lower ice deposit density, 0.96 g/cm^3 for the annual cap, application of which value would only lower our mass estimates. As noted earlier, the residual cap layers have some characteristics that are different from the current annual deposits, and there is a strong probability their bulk properties, including density, differ from the annual cap layer (Section 10).

8. Formation and degradation of the residual cap layers

In this section we apply the mapping results and change data to propose a synthesis of formation and degradation of the residual cap. We do not solve all the problems of the cap

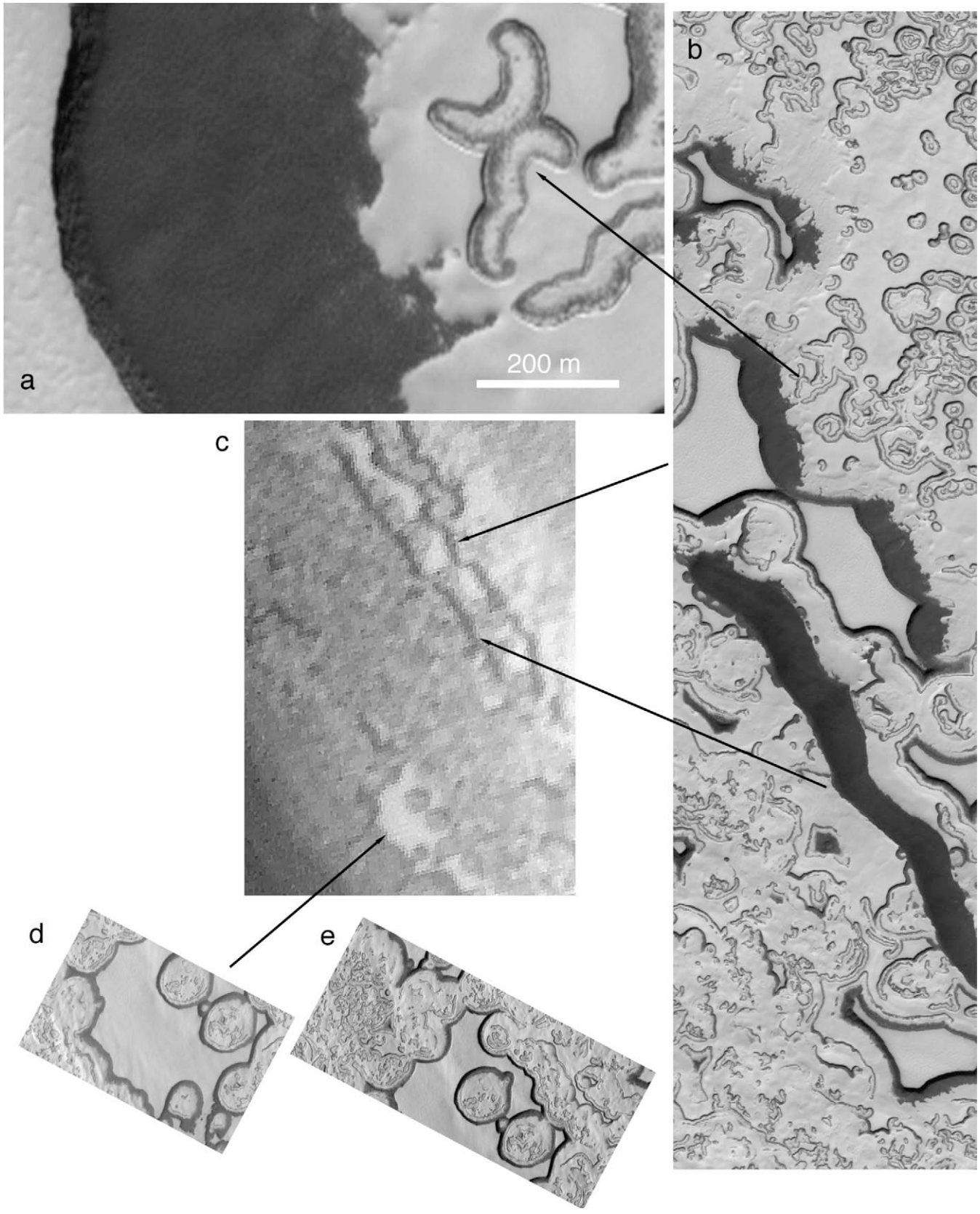

Fig. 16. Comparison of Mariner 9 image DAS 06029803, $L_s = 328°$ with MOC coverage. (a) Portion of MOC image M14-00542, 86.7° S, 344.2° W, $L_s = 332°$. (b) Larger portion of the M14-00542 image. (c) Mariner 9 image. (d) MOC image M15-00205, 87.0° S, 342.1° W, $L_s = 346°$. The two largest depressions are about 1100 m across. (e) MOC image E14-00862, $L_s = 340°$. In (b), north is to upper right.

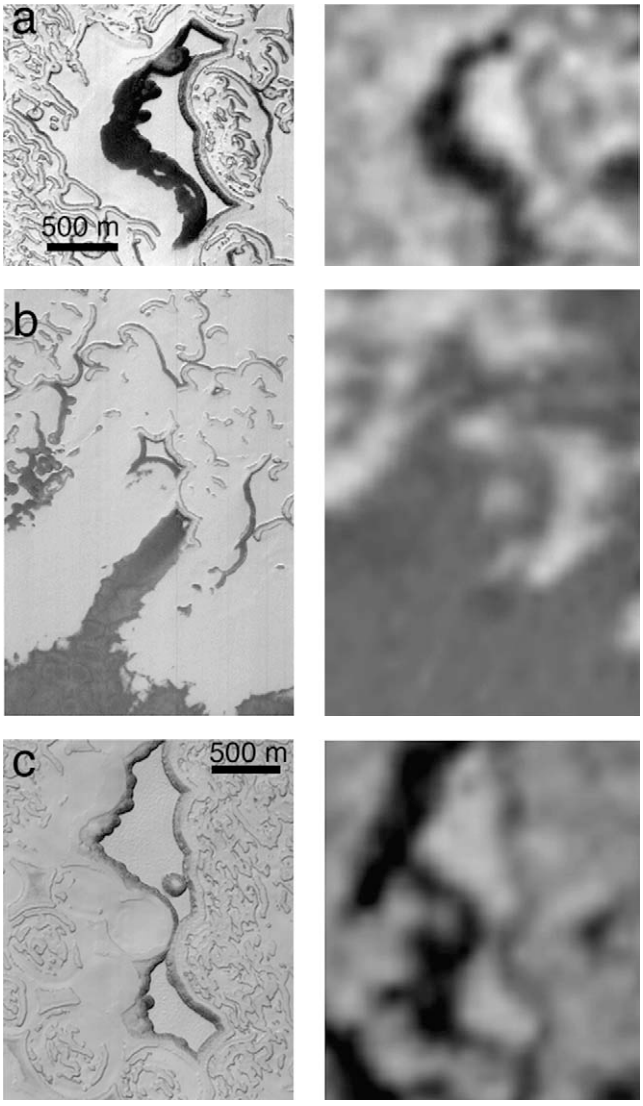

Fig. 17. Details of Mariner and MOC common coverage. Right side: Mariner 9 image DAS 09878689, $L_s = 357°$. (a) MOC image E15-01361, 86.3° S, 2.9° W, $L_s = 2.2°$. Mesa of unit A with dark region to the left, surrounded by complexly eroded unit B. Mariner 9 image shows the same basic mesa outline, with some difference in dark area. (b) MOC image E15-01361, 86.2° S, 3.8° W. Area is largely dark in Mariner 9 data, unit B layer dominates the MOC image. (c) MOC image E12-00825, 86.5° S, 358.2° W, $L_s = 304°$. Mesa in unit A surrounded by unit B. The Mariner 9 image may show a slightly larger connection between the two mesas.

history and makeup, and summarize in Section 11 some of the unresolved issues.

8.1. Thickness of the residual cap

What is the thickness of the residual cap? A completely satisfactory answer is probably not available from imaging remote sensing. However, there are many consistent indicators that it is a relatively superficial deposit compared to the 2 km or so of the polar layered deposits (Smith et al., 1999). There are no exposures of unit A (or any part of the residual cap material) with heights greater than about 14 m, and the survey of MOLA data on unit A mesas and other "outcrops" (Fig. 6) gives a tightly grouped set of thicknesses. These heights of unit A mesas are relative to the nearby covering of unit B, which has a minimum thickness of ~ 1 m. Thus we can describe the unit A thickness as 11 ± 2 m, with a maximum less than 15 m. In some areas the late summer images show very dark, differently textured materials near mesas of unit A, which may be the underlying polar layered deposits (Figs. 17a, 17b). Titus et al. (2003) infer the residual cap rests on water ice, some of which may be exposed over areas of more than 100 km^2 near residual cap edges. Byrne and Ingersoll (2003b) also note that thermal data indicate exposure of material much warmer than subliming CO_2 ice in some moats, which observation supports the photogeologic interpretation that units A and B rest on distinct materials. While we cannot rule out deeper residual cap materials, our measurements and extensive search of the images of the polar cap are consistent with the residual cap being at maximum ~ 15 m thick. This finding applies only to the remnants of unit A. Where the surface is unit B filling areas lost to unit A, the thickness may be much less. The observed gaps in the residual cap as observed by Mariner 9 also suggest areas of thin CO_2 ice cover.

8.2. Development of unit A

The layers in unit A represent some discrete depositional events or changes in deposition. The 2-m thickness of many, if not all, of the unit A layers indicates a considerable difference from the current ~ 1 m annual layer deposition at latitudes of 85°–87° S, assuming a CO_2 composition. The layers, 4 to 6 or even more in number, may indicate formation over multiple years or climate cycles.

All indications are that once the last layer of unit A was deposited those depositional conditions have not been repeated: unit A has since been stable or has been eroding. The polygonal troughs on the upper surface of unit A suggest the passage of some time interval adequate to induce fractures by thermal cycling or other contraction-related changes. The amount of erosion of unit A suggests, based on current rates of scarp retreat, $\sim 100+$ Mars y elapsed before the sequence of unit B was initiated.

At some time after the formation of unit A, apparently over much of the area of the present residual cap, degradation started. This erosion is manifested chiefly by the large circular depressions, curled depressions, and linear depressions with curled segments and ends (Figs. 3 and 5). Thomas et al. (2000) noted that the surface of (what we now call) unit A showed shallow, subtle depressions, or sags, that might be the precursors to the steeper-walled depressions we see backwasting at present. Byrne and Ingersoll (2003b) endorsed some role for sags as precursors to the more prominent depressions. The mapping exercise for this work has shown that sags and other indications of collapse from the bottom are common throughout the exposure of unit A (Fig. 3) as well as unit B. Features such as that in

Figs. 3f, 5a, and 5i indicate that material can be removed by heating from below, or that compaction has occurred, causing formation of depressions with locally greater slopes than the surrounding surface.

Steeper slopes in sags may be heated somewhat more by the Sun than horizontal surfaces, but this may not be the entire story of transforming sags or smooth depressions into the steep scarps that bound most depressions. The sag slopes are only a few degrees: a few m drop out of ~ 50 m horizontal, ~ 5°. At summer solstice, the Sun has an incidence angle of about 62° on a horizontal surface; on a 5° north-facing slope at noon the incidence is 57°. The difference of incident flux per area for the two cases is only about 16%. This ratio is less at other times of day. Given the apparent high stability of the top surface, it would seem more probable that the action of the sags is to introduce fractures and exposures of different scattering properties to the incident sunlight. The apparent longevity of the upper surfaces of both units A and B strongly suggest that neither is close to a threshold albedo, as intrinsic variations (implied by behavior of cap and atmosphere including dust loading) would bring the surface above and below the threshold frequently. The south facing ramps of the curled depressions (Byrne and Ingersoll, 2003b) and of the fingerprint terrain do suggest there are some insolation threshold effects on whether a steep, backwasting slope can be formed. However, these slopes are developed in what we would call disturbed parts of units A and B.

Sags suggest densification at depth or loss of material and collapse due to overburden weight. If loss of material by sublimation is occurring, the venting of CO_2 is passive compared to that postulated in some parts of the annual cap (Kieffer, 2003) as there are no indications of local vents or scattering of debris or other effects caused by release of pressurized CO_2. Loss by heating from below implies a warmer substrate, which would most likely be water ice precipitated and thermally held at temperatures well above the CO_2 condensation point for these pressures (Jakosky and Haberle, 1990). If the sags occur by parts of the layers losing porosity, but otherwise not suffering much sublimation, the required heat input might be much less. Sags also occur in some of the thicker unit B regions.

The orientations of the curls, the azimuth of a line from the steep side to the cusp (right to left in Fig. 5b), are plotted in Fig. 18. These data cover more territory than the local study reported by Byrne and Ingersoll (2003b), and include unit B curls, and show a much greater range of azimuths. Our results are consistent in the area of data overlap, but the broad range of orientations indicates some effects in addition to greatest solar elevation.

Whatever way the depressions were initially formed in unit A, the expansion of nearly circular forms has removed a significant fraction of the deposit. Perhaps the most striking aspect beyond the near-circularity of many of these depressions, is their size relative to their depth. The backwasting rate in many must have exceeded any downwasting by a large factor: the radius of the depression (as large as several hundred m) compared to the small net amount (< 1 m?) removed from the top. Either the process of collapsing scarps during backwasting, or the character of the lower layers of unit A, or both, have led to the basal patterned debris ramps, which may have retreated along with the upper scarps.

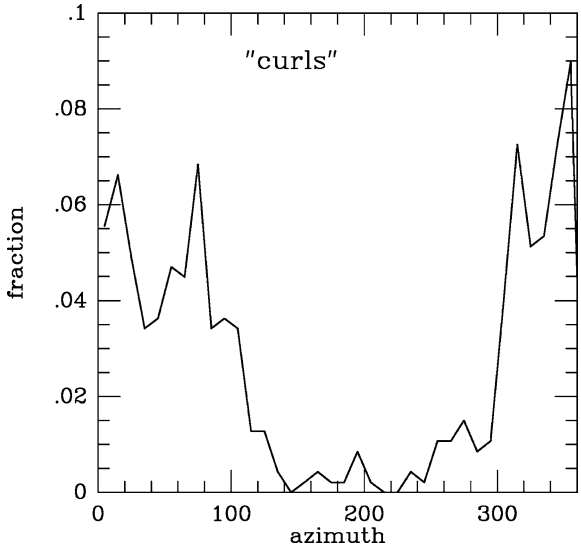

Fig. 18. Azimuths of curl depressions. Azimuth is direction from smooth side to cusp, right to left in Fig. 5b. Note there is nearly a 180° range of frequent azimuths.

While backwasting dominates most of the apparent removal of unit A, there are remnants of unit A that lack the flat upper surface (see Figs. 5e and 10a) and indicate that these examples of unit A suffered collapse or downwasting after significant backwasting. Figure 19 shows three stages in the degradation of unit A: Fig. 19a shows the familiar mesa formed by scarp retreat with debris aprons extending nearly 200 m in some parts. Figure 19b shows a remnant having largely collapsed into a low hill before being partly covered by unit B, which is now being stripped. This type of hill with what may be described as a "peel" of unit B is common on the south residual cap. Less common, but scattered between longitudes 350° W to 80° W, and between latitudes 85° and 86° (minor exceptions as far south as 86.5°) are forms such as those in Fig. 19c. Here the scalloped outline is familiar, but it is lower than the surrounding unit B surface. The unit A mass here has apparently nearly completely collapsed, creating an inversion of relief: what was higher is now lower.

To form such inverted relief, unit A at some point must have responded very differently from unit B to imposed thermal (or other) erosional influences. This response also is different from the usual backwasting of the unit. The timing of the effective collapse of the mesas is not well constrained. The interpretation of inverted relief depends upon the arcuate scarps forming in material in stacks of similar form to the 10–13 m high ones seen today. After the cessation of the backwasting, and possibly during some of the erosional episodes of unit B, or even after the backwasting

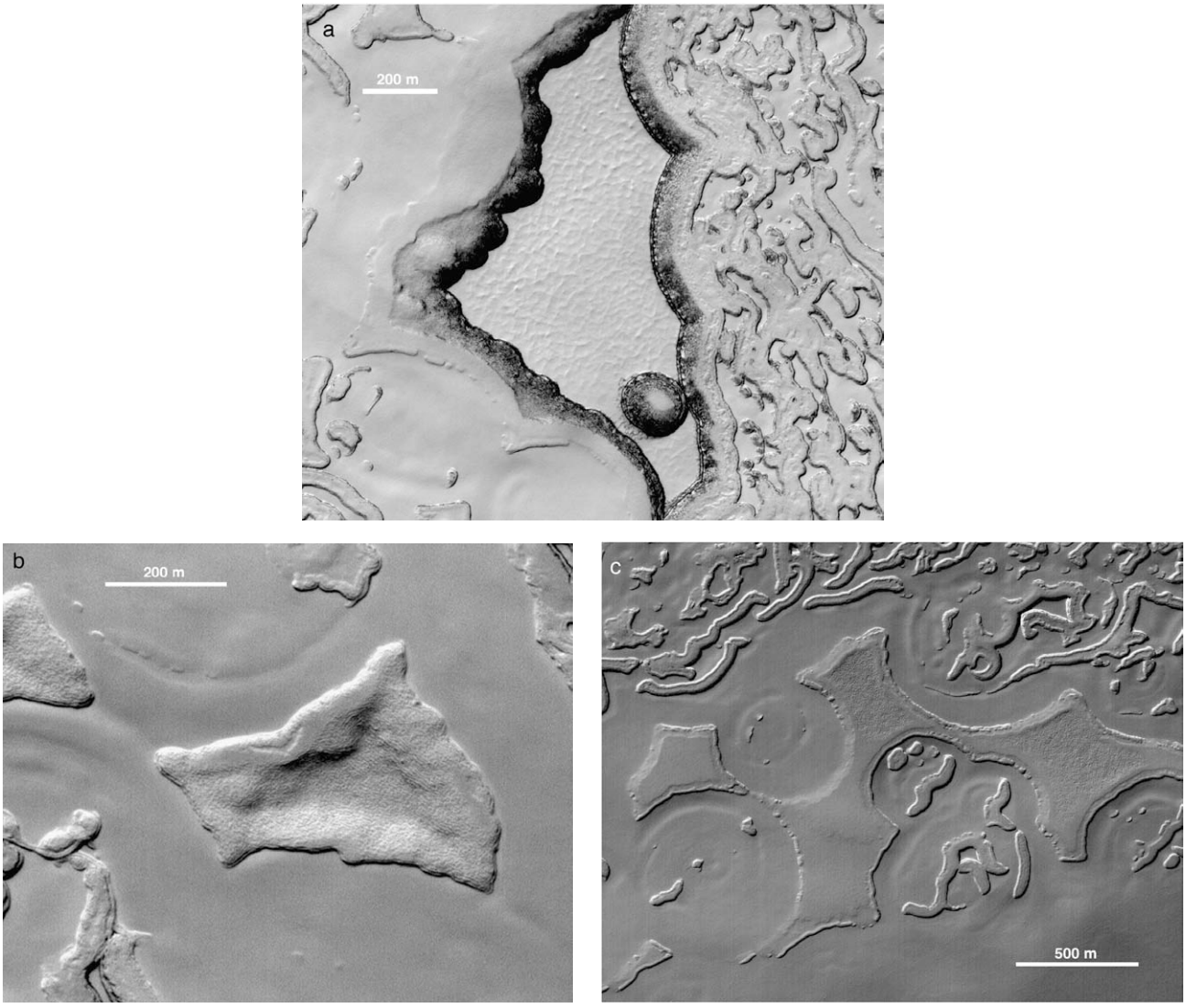

Fig. 19. Sequence of degradation of unit A relative to unit B. (a) Unit A mesa formed by backwasting. MOC image E12-00825, 86.5° S, 358.4° W, $L_s = 303°$, nazim = 237°. (b) MOC image M12-00655, 86.9° S, 81.0° W, $L_s = 295°$, nazim = 293°. (c) MOC image M09-04151, 86.3° S, 354.4° W, $L_s = 245°$, nazim = 309°. Arcuate outline, best interpreted as a former unit A mesa (see Figs. 3, 12, 17), is lower than the surrounding exposure of unit B. Sunward-facing slopes give key to relative heights. The difference in heights is subtle, of order one m.

erosion of A but before the deposition of some B layers, unit A could have collapsed. We have found that unit A currently erodes about 50% faster than unit B. This rate would not serve to impose topographic inversion, but does signify that A does have different properties from B that might allow very different behaviors over some thermal thresholds. Schematic cross sections of the formation of unit A mesas and inverted relief are shown in Fig. 20. Note that the backwasting is shown only in steps b and f of Fig. 20. Step c is deposition, and d and e are the collapse of unit A, which is a process distinct from measured backwasting (Section 5).

There are relatively few very small, steep walled depressions in unit A (Fig. 7a). The circular depressions have very few examples less than 200 m across. By contrast, the unit A curls have a mean size of 191 ± 57 m ($n = 314$). This difference might represent a generational difference, because the current backwasting rates measured in the different features are indistinguishable (Table 1).

8.3. Unit B development

The development of unit B is no less complicated and surprising than that of unit A. While unit A largely can be regarded as a single entity that formed (probably over several years) and suffered erosion, unit B clearly contains depositional events interrupted by erosion. (As noted above, it may be more properly described as erosion interrupted by depositional episodes; Fig. 15.) The primary tell-tales are the multiple thicknesses of unit B, the bimodal distribution of moat widths, and the relative thicknesses of materials making the moats.

As noted above, a surprising aspect of the formation of unit B is that although it is younger than unit A, actually

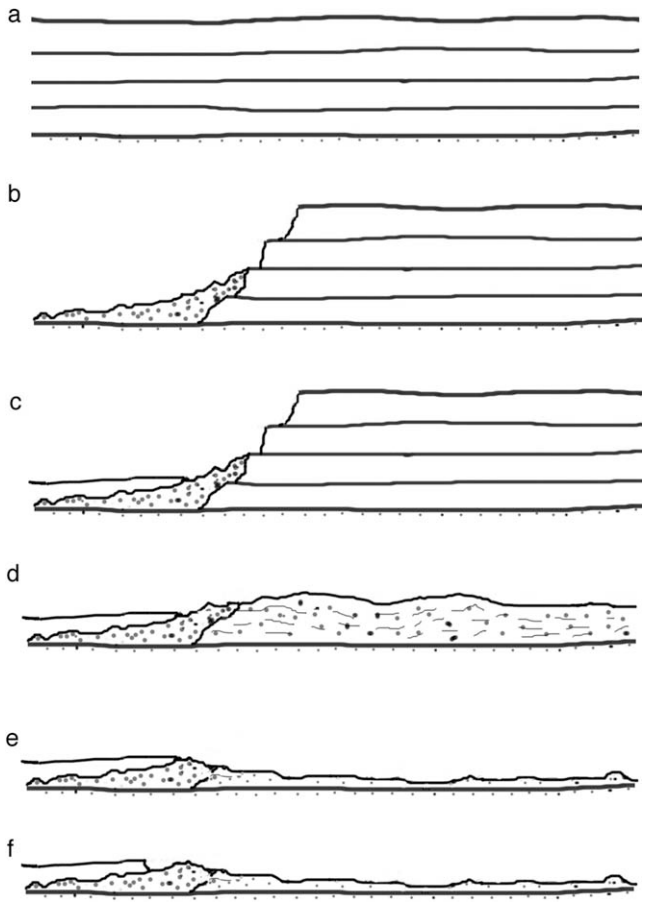

Fig. 20. Schematic sequence for development of inverted relief. (a) Deposition of several layers of unit A. (b) Backwasting of unit A, with debris on lower slopes. Scarp is similar to those in Fig. 3. (c) Deposition of a layer of unit B. Compare to Figs. 5d, 5h. (d) Downwasting or collapse of much of remaining unit A materials. Compare Figs. 5e and 19b. (e) Further downwasting, producing an inversion of relief. (f) Backwasting of unit B cover to produce scarp. Compare to Fig. 19c.

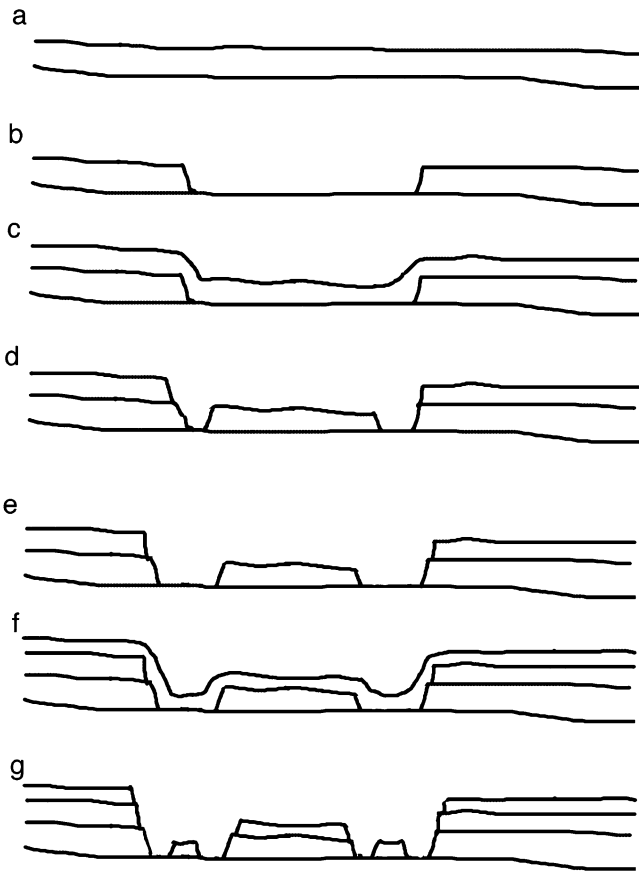

Fig. 21. Schematic of development of depression moats in unit B. (a) Deposition of a layer of unit B. (b) Backwasting of depression in unit B layer. (c) Deposition of second unit B layer. (d) Backwasting of steeper parts of unit B stack. (e) Further backwasting enlarges the moat. (f) Deposition of third unit B layer. (g) Backwasting of steeper sections resumes, leaving two scales of moats, as seen in Fig. 10c.

younger than a considerable period of erosion of unit A, it apparently was either not deposited on the upper surface of unit A, or did not survive there. This conclusion follows from the very different surfaces of units A and B, the different small depression types in the upper layers of A and of B, the different thicknesses of the top layers of A and B, and the different erosion rates of the units. The key element here may be its lack of survival, rather than possible non-deposition, as discussed in Section 10.

Unit B has up to three layers, and its most distinguishing topography is the population of moats within its depressions and between it and unit A outcrops (Figs. 3, 5, 7). The very strong bimodality of depression moat widths, the widespread occurrence of medial material in moats (Fig. 10) and the lack of moats within small depressions show there has been a start-stop process in eroding the depressions in unit B. A possible scheme is shown in Fig. 21. This sequence is common on the residual cap, but is not ubiquitous, as the region dominated by fingerprint terrain lacks such forms. The last depositional event, responsible for the medial deposits and smallest moats seen in Figs. 10c, 10e, appears to be even thinner than the other unit B layers. It does not present any scarps either tall enough or sharp enough to cast shadows that give a reliable height measure.

The consistent spacing and sizes of the fingerprint depressions, as well as their occurrence in a central region (Fig. 9) suggest that their initiation was different from the seemingly random arrangement of the curls in unit A and most other depressions in unit B. The consistent orientation of the fingerprints, which is not a constant compass azimuth (Fig. 22), suggests a structural origin. In fact, some fingerprint depressions have narrow (< 5 m wide) markings extending from their ends which suggest fractures or cracks. The indication that rather subtle sags may initiate scarp formation suggests that very little surface offset, or opening of cracks is required to set in motion scarp retreat. The probable short time required to form the present widths of the fingerprint depressions and their consistency in direction and size indicate the operation of some condition or event over an area of $\sim 10{,}000$ km^2 during a restricted time interval. It is not known what this event could be. There are sets of smaller parallel depressions; these appear to involve only one layer

and show much more influence of local topography on their directions, possibly because they may tend to form in areas of greater local relief.

Unit B also has curled depressions; those mapped have a mean size of 122 ±75 m; ($n = 362$). These depressions also have some ramps in the cusp portion, although their appearance is somewhat less symmetric than many of the ramps and cusps of unit A curls. Although there is a great deal of overlap in size with the unit A curls, and some of the unit B curls are up to 280 m across, the average smaller size and the smaller rate of retreat of unit B suggest these forms could have expanded during the same interval as curls in unit A.

8.4. Seasonal changes

Observations of changes within one season enhance the interpretation of the degradation of the layers. Between 86° and 87° S, the upper surfaces, steeper slopes, and floors of depressions, including the moats, present a fairly uniform brightness in MOC NA images until an L_s of about 280°. Through $L_s \sim 310°$ (this date varies with locale) the steeper slopes start to show darkening relative to the flatter surfaces. After $L_s \sim 320°$ floors of moats become relatively dark. The tracking of the initial darkening of steep walls is possible only with the higher resolution images (< 3 m/pixel); moat darkening can be seen in much lower resolution images. On a much broader scale, significant changes to residual cap outliers at slightly lower latitudes can be observed after $L_s = 300°$ (James et al., 1979, 1992). The albedo of the residual cap measured in MOC WA images peaks at about $L_s = 280°$ and then decreases gradually through the summer

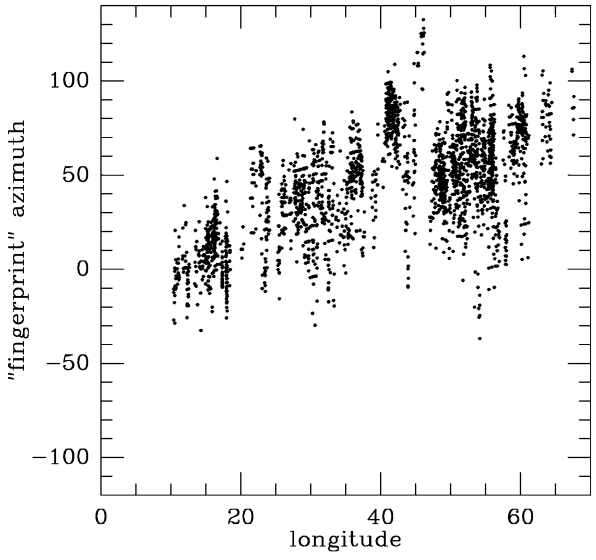

Fig. 22. Azimuths of fingerprint depressions. Azimuths, measured from steep side to gentle side (right to left, slightly up, in Fig. 8d) as a function of longitude. The azimuths on average rotate in concert with the longitude. The directions of these features are not primarily dependent upon compass direction (i.e., solar exposure) but represent a continuous trend across over 200 km distance.

(James, 2001). The darkening of the walls may contribute to this effect in the 240 m/pixel WA images.

8.5. Other influences on degradation of the residual cap

Most of the degradational forms in both units A and B originate from the expansion of depressions by backwasting. However, some expand at least in part under the action of the wind. Examples are shown in Fig. 23, and a map of elongation directions is presented in Fig. 24. These elongate forms affect both units A and B, and are initiated at both positive and negative relief forms. Those emanating from the large circular depressions in unit A have affected only the top layer and leave a debris covering similar to that found on surrounding slopes (Figs. 5d, 23c). Their expansion has kept pace with the opening of the depressions, although the ratio of length to source depression diameter varies by a factor of two (Fig. 23). The very largest depressions in this area do not show these tails. The inferred wind directions are partly consistent with summer, off-pole flow turned to a retrograde (toward the west) direction (French and Gierasch, 1979). The ones in Fig. 23c do not fit this pattern (the most right group in Fig. 24). They do, however, follow the local slope of about 1.5°. Other elongate forms, including those in Figs. 23a, 23b, point into troughs from the residual cap area, and would appear to be related to slope winds (see Howard (2000)). Our survey of these forms is incomplete. In fact, many of the markings visible in the Mariner 9 images (Figs. 16 and 17) appear to be wind-controlled exposures of the substrate in the lee of unit A mesas. These were not included in the preliminary tabulation mapped in Fig. 24.

The role of the wind in forming the elongated depressions might be to remove material physically, or to enhance transfer of atmospheric heat to the frost layers, or to induce modification of the frost surface texture. Physical removal of material is inferred to occur in some low latitude wind streaks (Greeley et al., 1992). Relatively simple modeling might disclose if it is possible that topographically modified flow might enhance transfer of sufficient atmospheric heat to the frost layers. More sophisticated modeling may be required to indicate if the expected flow modifications due to the topography could change the surface texture sufficiently to alter the effective albedo. These last two possible mechanisms are interrelated.

8.6. Collapse, "Escher" terrain and depositional variations

Sags and collapse (Fig. 3f) are only part of a spectrum of forms that indicate further complexities in the deposit history and pose considerable interpretive challenges. Instances where an upper surface appears to merge with a lower, apparently later surface, abound (Fig. 25a), and have been informally termed "Escher" terrain because of the seemingly contradictory geometry. Usually the transition to the

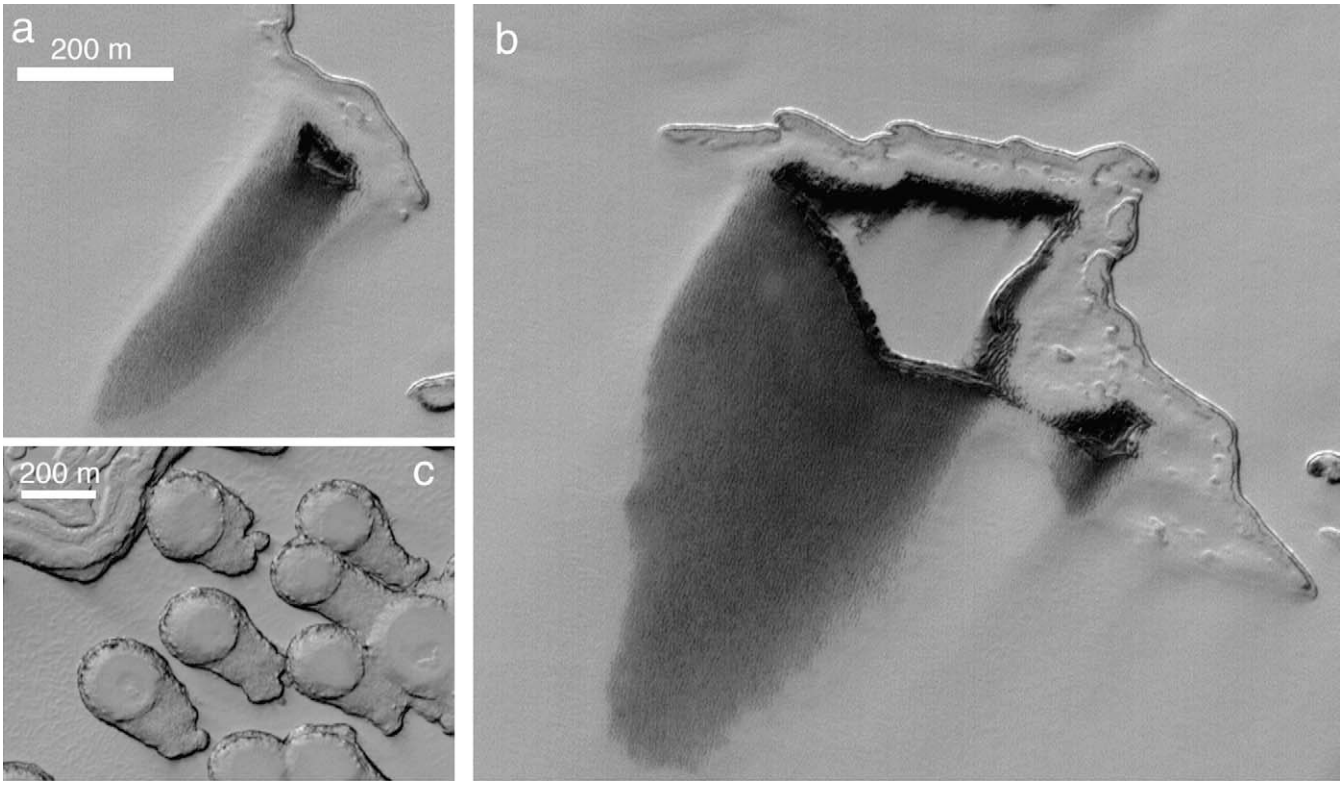

Fig. 23. Wind modification of units B and A in residual cap. (a) MOC image E14-00295, 86.2° S, 6.9° W, $L_s = 337°$, nazim = 230°. (b) MOC image E14-00295. 86.2° S, 7.3° W, $L_s = 337°$, nazim = 230°, same scale as (a). (c) MOC image E11-01186, 86.8° S, 347.5° W, $L_s = 284°$, nazim = 280°.

lower level surface is not a linear ramp, but includes a subtle break in slope from a convex to concave slope (near #3 in Fig. 25a). The problem is that in the area of #3 the interpretation would be collapse, but between #4 and #1 it would be erosion followed by deposition of unit B. Both processes could apply if the deposition of unit B included feather edge deposition against some of the higher remnants that did not subsequently form moats. The deposition of unit B on debris from unit A shown in Fig. 10d leaves a break in slope similar to that shown at #3 in Fig. 25a. Feather edge deposition of the later units might explain the topography, but this scenario might require that the feather edge deposition survive in only certain instances, as yet unknown. Figure 25b shows a simple generation of an Escher terrain example. Here there is no evidence of separate deposition forming the ramp and moat-like form.

A further complication to simple layering are features in unit B such as shown in Fig. 10c. The upper layers, bounded by a brighter scarp, are being removed from an underlying surface whose form influences the topography in the overlying layer. These forms also appear to be "Escher" topography, in that the left most surface of Fig. 10c appears to wrap around to the next lower (middle) level (out of the image portion shown). MOLA profiles across this type of form show them to be steps, 30–40 m high, the extra height gained in less than two MOLA footprints (less than ~ 600 m). This is much greater topography than is associated with any of the layer forms (depressions; visible layers), and may well

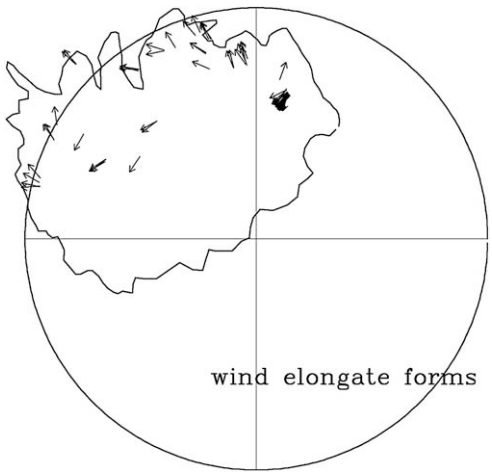

Fig. 24. Wind directions inferred from elongate forms in residual cap such as those in Fig. 23. Circle is 85° S, 0° longitude is at top.

be caused by the topography of the polar layered deposits under the residual cap deposits. These step-like forms have been found chiefly between longitudes 40° and 65° W and latitudes 84.5° S and 86° S.

Some more complications on a simple scheme are shown in Fig. 25c. Here we see rounded, isolated patches of two-layer deposits displaying both steep scarps as well as rounded, convex slopes to an underlying, evidently different, material. These might be the result of variable deposition, or might be erosional forms.

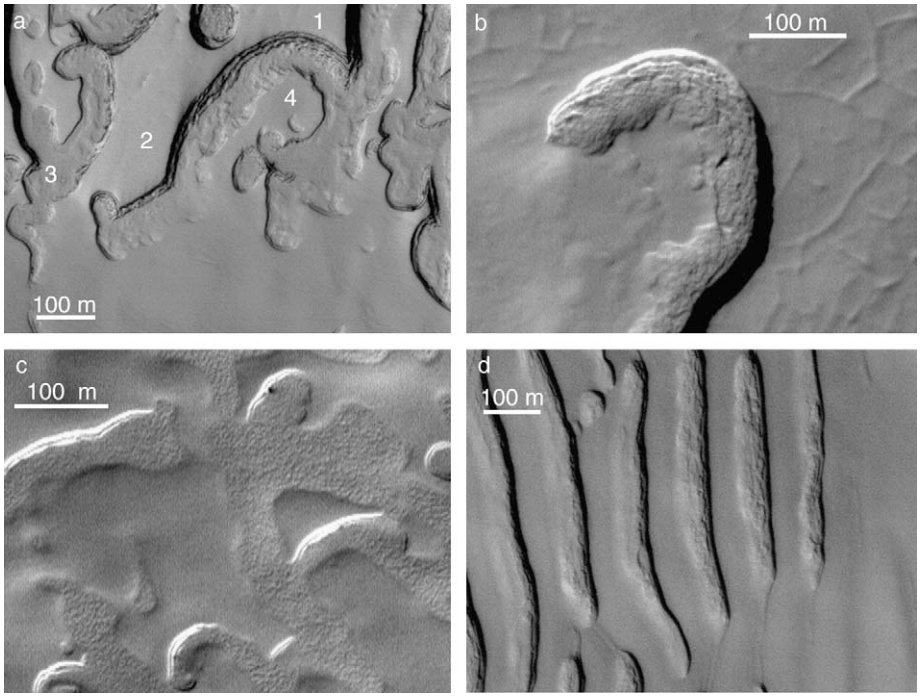

Fig. 25. "Escher" terrain and other depositional or erosional complexities. (a) "Escher" terrain. Upper section ramps to a surface that is lower and appears younger than the taller layer stack. Follow upper surface from #1 to #3. Subtle break in slope occurs at #3. #4 and #1 are different materials at different levels, but are connected by a smooth surface interrupted only by the subtle break in slope. MOC image M12-01026, 85.9° S, 51.1° W, $L_s = 297°$. (b) Curl feature in unit A with typical collapse and ramp form that resembles other "escher" terrain. Compare to (a). MOC image M09-00609, 86.9° S, 6.8° W, $L_s = 236°$. (c) Layer outliers showing possible collapse effects on thicknesses, or uneven deposition. Note the feathering of the layers in the exposure in the right center. MOC image M09-05440, 86.9° S, 335.2° W, $L_s = 249°$. (d) Fingerprint terrain with thin linear features extending toward the bottom of image area, suggesting structural influence on location. MOC image M08-01818, 87.0° S, 5.1° W, $L_s = 219°$.

8.7. Physical nature of the residual cap materials

While it is reasonably certain that CO_2 ice is a major component of the residual cap layers, it is also clear that the deposits encompass substantial physical, and perhaps compositional, variety. Properties of the annual CO_2 deposit depend in part on grain size at deposition, amount and particle size of included dust and water ice (Hansen, 1999), and the evolution of these properties as insolation is absorbed during the spring (Kieffer et al., 2000; Kieffer, 2003). The relatively dark "cryptic" region of the annual cap may be slab CO_2 (extremely large grain size) that allows radiation to penetrate nearly a m into the ice (Kieffer et al., 2000). Not all of the annual cap is of this nature, and as the spring progresses, there are a variety of possible avenues for loss of the dust in concert with sublimation of CO_2 (Kieffer, 2003). The residual cap deposits have several characteristics that would have to be accommodated in a comprehensive physical model: (1) The upper surfaces of both units A and B appear very stable, neither accumulating or losing significant material. (2) Scarps in units A and B receded at different rates. (3) The exposed interiors of the layers in the steep walls have lower late summer albedos than the upper surfaces. (4) Some loss of material may occur at depth (to form sags).

To satisfy (1) above, the material either has to have an albedo sufficiently high that CO_2 will not reach temperatures where significant loss by sublimation occurs, or it must be compositionally distinct. Characteristic (2) could be satisfied in several ways. The simplest is the deposits have different porosities. This condition would provide different masses per unit area exposed to insolation, which with optical properties otherwise equal, could allow for faster retreat of the more porous material. Alternatively, there might be different amounts of included dust that affect the albedo and thus the absorption of heat. The debris formed around unit A scarps and left after mesas collapse suggest inclusion of some materials that may not be present in unit B (unit B does not leave such debris). For (3), we simply need a difference between the last deposition of CO_2 ice during the layer deposition (one winter?), or an effect of burial that renders the deeper parts of a layer more subject to radiation absorption, such as compaction and sintering. Modification by burial is probably not the explanation, as the tops of layers that have been buried by other layers (including many cycles of annual layers) retain their higher albedo in the outcrops of layer steps. For (4) there would have to be a plausible amount of heat conduction from below. If these are layers of CO_2 deposited over water ice rich layers that equilibrated at substantially higher temperatures, then there could be heat flow from below. This is essentially part of the situation modeled by Jakosky and Haberle (1990).

The morphology and change rates do emphasize that the residual cap either has admixtures of different materials, or has different physical forms of a dominant component

(CO_2?) that can respond very differently to the imposed range of climate. Any modeling of residual cap processes will need to consider this range.

9. What are the climate changes or cycles responsible for deposition and erosional cycles in the residual cap?

The depositional and degradational environment on the residual cap has changed many times, not necessarily in a regular, cyclic manner. The interpretations and measurements summarized by Fig. 15 indicate short period changes (depositional events) separated by one to a few Mars decades. It is also inferred that a different set of depositional events formed unit A perhaps ~ 150 Mars y ago.

Climate changes on decade to centuries scales cannot be related to orbital forcing: the shortest period is likely $\sim 5 \times 10^4$ y (Laskar et al., 2002; Head et al., 2004). The lack of large thermal reservoirs such as oceans that can feed intermediate time scale climate oscillations suggests that changes in the climate might be due to variations in atmospheric dust loading or in the global surface albedo caused by dust deposition. Although there is nearly continual dust activity (Cantor et al., 1999, 2002), planet-encircling dust events are much less frequent. They can occur on decadal time scales (Martin and Zurek, 1993), at least within the last several decades of good terrestrial and spacecraft observations. Recovery of the ground albedo (Christensen, 1988; Smith, 2004), and the general circulation from these events is rapid, of order a Mars year, compared to the intervals we have inferred between the periods of erosion of residual cap. Thus, a temporal scale association of large dust events and short depositional events may be reasonable.

How would global dust events foster unusual depositional episodes? Effects of atmospheric dust may be indirect. For example, a change in dust loading may produce a change in the winter polar vortex (McConnochie et al., 2003), which may in turn affect the deposition mechanism of CO_2 or the pattern of CO_2 redistribution by surface winds. Widespread dust deposition can cause global daytime cooling of a few K (Smith, 2004) which might also alter CO_2 deposition or sublimation rates. The balance of sublimation on the caps is strongly dependent on the albedo of the ice (Toon et al., 1980; Paige and Ingersoll, 1985), which can be affected by dust content (Bonev et al., 2002). Our observations that the upper surfaces of the residual cap deposits are effectively stable suggest that if units A and B are largely CO_2, then they apparently have been deposited with surface albedos sufficiently high to essentially stabilize their upper surfaces. Once breached, however, by fracturing or collapse, the albedo is low enough to allow sublimation. The key difference in the deposits of the residual cap from a typical seasonal CO_2 cover appears to be deposition with textures that preserve a high albedo, in contrast to some of the complex changes in optical properties seen in the usual annual CO_2 cap (Kieffer et al., 2000).

The deposition of unit A occurred under conditions that apparently have not been repeated for more than ~ 150 Mars y. We may speculate that this deposition was coincident with the Maunder minimum that may have seen slight reduction in solar irradiance from ~ 1645–1715 (Shindell et al., 2001), or ~ 150 to 190 Mars y ago. Apart from the difficulty of establishing a mechanism for the possible connection to a very subtle effect, the deposition of unit A probably was short compared to the possible duration of the effect.

10. What are the layers?

What is the time interval or event responsible for the individual layers in the residual cap? As noted above, the residual cap layers differ from the current annual winter deposit in their surface characteristics, such as albedo, and their greater thicknesses, ~ 2 m. The mass deposited during a winter depends primarily on the radiative budget; some variation may be possible by wind transport. Year-to-year changes in the amount of CO_2 deposited during the winter appear to be small. Viking Lander pressure measurements for two Mars years were very repeatable (Tillmann, 1988). The recession pattern of the annual cap from long term Earth based observations and from spacecraft data shows only modest variation (James et al., 1979, 1992; Bonev et al., 2002). Thus, obtaining much thicker deposits in a winter probably requires a change in the mean density (porosity) of the deposit. The current amounts of winter deposition of CO_2 ice at latitudes above 85° S can be predicted with radiative models and reference to atmospheric pressure changes. Results of Kieffer et al. (2000) give values around 1000 kg/m^2 at 80° S, and slightly higher estimates on the residual cap region. For completely solid CO_2 ice with a density of 1.5 g/cm^3, the residual cap mass loading estimate of 1000 kg/m^2 implies a deposit depth of 0.7 m. A 2 m thick deposit of the same mass loading would have to have a porosity of slightly over 65%. For snow deposits this porosity might be unusual only in being low. Thus, if conditions allowed the same mass to be deposited in a form different from surface slabs, probably with inclusion of a significant fraction of porous snowfall, then a single winter's deposition might form a residual cap layer. Deposits with more highly porous material and smaller grain sizes might be expected to have the higher albedos of the residual cap materials.

While a one-year, 2-m layer may be possible, we may approach the question from the other direction: can two-m layers be multi-year units? Whatever their makeup, at least the upper layers of unit A and the thicker ones of unit B, appear quite homogeneous. This uniformity is most clearly demonstrated in the evenness and length of many of the steps in the walls of scarps in unit A. If the individual layers formed over more than a few years, they would have to consist of some form of residue from the annual deposition, yet lack significant annual discontinuities. A simple partial residue

of the annual cap that fails to sublimate, several years in a row, seems unlikely on two counts: First, there would have to be a very fortuitous thermal balance only allowing part of the CO_2 to sublimate, and leave a fraction behind. Second, this would have to occur several years in a row, and leave a total deposit (one layer of unit A or of unit B) that is of fairly even thickness over wide areas. A residue of sublimation that is small compared to the original deposit would more likely be some different composition from the bulk starting annual deposit. The rates of scarp retreat in the current residual cap seem inconsistent with H_2O ice (Malin et al., 2001), and at least consistent with CO_2. The simplest explanation may be that the layers are unusual single winter deposits, with the unit A layers having a different structure from the unit B layers, and both somewhat different from the typical annual deposit.

11. Unsolved problems

This study has, of necessity, left many problems unresolved. Perhaps the most serious photointerpretive problem is the uncertainty in discriminating between feather-edge deposition and some collapse effects, with the attendant possibility of major stratigraphic error. There is much work to be done correlating albedo changes from Mariner 9 to Viking to Mars Global Surveyor with features seen at high resolution. High-resolution thermal studies (for example, Thermal Emission Imaging System; THEMIS) may help in this area. The role of underlying topography in affecting the residual cap morphology, such as in Fig. 8c and the rows of mesas such as in Fig. 16, has not been investigated. The physical properties of CO_2 ice/frost need to be elucidated, as well as the microphysics of CO_2 deposition from the Mars atmosphere. What component of unit A results in the collapse debris morphology is unknown. Where the sublimated CO_2 goes is unknown. And, of course, we still do not know why the whole residual cap in the south is where it is.

12. Conclusions

The south residual cap is made up of two major layered units, deposited at different times, separated by a period of degradation. The maximum thickness, in the older materials, is less than 15 m composed of layers approximately 2 m thick. The younger unit has up to 3 layers, ~ 1 m in thickness. The older unit currently backwastes at 3.6 m/Mars y, the younger one at 2.2 m/Mars y. All forms in the south residual cap are currently undergoing backwasting. Erosion appears to be the norm for the residual cap, interspersed with periods of deposition. The difference of the residual cap materials from normal winter deposition might be as simple as inclusion of a greater than usual fraction of snowfall.

Acknowledgments

Ken Edgett targeted the change images as well as other south polar images, and provided extremely helpful discussions on many of the topics covered in this work. We acknowledge helpful discussions with R. Sullivan and J. Veverka. Technical assistance was provided by B. Carcich, L. Wei, R. Chomko, K. Consroe, and R. Kline. Tim Titus and an anonymous reviewer provided notable assistance. This work was supported by NASA.

References

Bibring, J.-P., Langevin, Y., Poulet, F., Gendrin, A., Gondet, B., Berthe, M., Soufflot, A., Drossart, P., Comes, M., Bellucci, G., Moroz, V., Mangold, N., Schmitt, B., the OMEGA Team, 2004. Perennial water ice identified in the south polar cap of Mars. Nature 428, 627–630.

Bonev, B.P., James, P.B., Bjorkman, J.E., Wolff, M.J., 2002. Regression of the Mountains of Mitchel polar ice after the onset of a global dust storm on Mars. Geophys. Res. Let. 29, 13-1–14-4.

Byrne, S., Ingersoll, A.P., 2003a. A sublimation model for martian south polar features. Science 299, 1051–1053.

Byrne, S., Ingersoll, A.P., 2003b. Martian climatic events on timescales of centuries: evidence from feature morphology in the residual south polar ice cap. Geophys. Res. Lett. 30, 29-1–29-4.

Cantor, B., James, P.B., Caplinger, M., Wolff, M.J., 1999. Martian dust storms: 1999 Mars Orbiter Camera observations. J. Geophys. Res. 106, 23653–23688.

Cantor, B., Malin, M., Edgett, K.S., 2002. Multiyear Mars Orbiter Camera (MOC) observations of repeated martian weather phenomena during the northern summer season. J. Geophys. Res. 107, 3-1–3-8.

Christensen, P., 1988. Global albedo variations on Mars: implications for active aeolian transport, deposition, and erosion. J. Geophys. Res. 93, 7611–7624.

Flammarion, C., 1892. La planete mars et ses conditions d'habitabilite, v. 1. Gauthier–Villars et Fils, Paris.

French, R.G., Gierasch, P.J., 1979. The martian polar vortex: theory of seasonal variation and observations of eolian features. J. Geophys. Res. 84, 4634–4642.

Greeley, R., Lancaster, N., Lee, S., Thomas, P., 1992. Mars aeolian processes, sediments, and features. In: Kieffer, H.H., Jakosky, B.M., Snyder, C.W., Matthews, M.S. (Eds.), Mars. Univ. of Arizona Press, Tucson, pp. 730–766.

Hansen, G.B., 1999. Control of the radiative behavior of martian polar caps by surface CO_2 ice: evidence from Mars Global Surveyor measurements. J. Geophys. Res. 104, 16471–16487.

Head, J.W., Mustard, F., Kreslavsky, M.A., Milliken, R.E., Marchant, D., 2004. Recent ice ages on Mars. Nature 426, 797–802.

Howard, A.D., 2000. The role of eolian processes in forming surface features of the martian polar layered deposits. Icarus 144, 267–288.

Jakosky, B.W., Haberle, R.M., 1990. Year-to-year instability of the Mars south polar cap. J. Geophys. Res. 95, 1359–1365.

James, P.B., 2001. MOC observations of the martian south polar cap in 1999–2000. J. Geophys. Res. 106, 23635–23652.

James, P.B., Briggs, G., Barnes, J., Spruck, A., 1979. Seasonal recession of Mars' south polar cap as seen by Viking. J. Geophys. Res. 84, 2889–2922.

James, P.B., Kieffer, H.H., Paige, D.A., 1992. The seasonal cycle of carbon dioxide on Mars. In: Kieffer, H.H., Jakosky, B.M., Snyder, C.W., Matthews, M.S. (Eds.), Mars. Univ. of Arizona Press, Tucson, pp. 934–968.

Kieffer, H.H., 1979. Mars south polar spring and summer temperatures: a residual CO_2 frost. J. Geophys. Res. 84, 8263–8288.

Kieffer, H.H., 2003. Behavior of solid CO_2 on Mars: a real zoo. In: 3rd Mars Polar Conf. Abstract #3158.

Kieffer, H.H., Chase, S.C., Martin, T.Z., Miner, E.D., Palluconi, F.D., 1976. Martian north pole summer temperatures: dirty water ice. Science 194, 1341–1344.

Kieffer, H.H., Titus, T.N., Mullins, K.F., Christensen, P., 2000. Mars polar spring and summer behavior observed by TES: seasonal cap evolution controlled by frost grain size. J. Geophys Res. 105, 9653–9699.

Kuiper, G.P., 1957. Visual observations of Mars. Astrophys. J. 125, 307–317.

Laskar, J., Levrard, B., Mustard, J.F., 2002. Orbital forcing of the martian polar layered deposits. Nature 419, 473–477.

Leighton, R.L., Murray, B.C., 1966. Behavior of carbon dioxide and other volatiles on Mars. Science 153, 136–144.

Lowell, P., 1895. Mars. Houghton Mifflin, Boston.

Malin, M.C., Caplinger, M.A., Davis, S.D., 2001. Observational evidence for an active surface reservoir of solid carbon dioxide on Mars. Science 294, 2146–2148.

Martin, T., Zurek, R., 1993. An analysis of dust activity on Mars. J. Geophys. Res. 98, 3221–3246.

McConnochie, T.H., Conrath, B.J., Banfield, D., Gierasch, P.J., Smith, M.D., 2003. The martian polar vortex: interannual variability and comparisons to Earth. Bull. Am. Astron. Soc. 35.

Murray, B.C., Soderblom, L.A., Cutts, J.A., Sharp, R.P., Milton, D.J., Leighton, R.B., 1972. Geological framework of the south polar region of Mars. Icarus 17, 328–345.

Paige, D.A., Ingersoll, A.P., 1985. Annual heat balance of martian polar caps: Viking observations. Science 228, 1160–1168.

Paige, D., Wood, S., 1992. Modeling the martian seasonal CO_2 cycle. 2. Interannual variability. Icarus 99, 15–27.

Paige, D., Herkenhoff, K., Murray, B., 1990. Mariner 9 observations of the south polar cap of Mars: evidence for residual CO_2 frost. J. Geophys. Res. 95, 1319–1335.

Shindell, D.T., Schmidt, G.A., Mann, M.A., Rind, D., Waple, A., 2001. Solar forcing of regional climate change during the Maunder minimum. Science 294, 2149–2152.

Slipher, E.C., 1962. Mars: The Photographic Story. Sky Publishing, Cambridge, MA.

Smith, M.D., 2004. Interannual variability in TES atmospheric observations of Mars during 1999–2003. Icarus 167, 148–165.

Smith, D.E., 18 colleagues, 1999. The global topography of Mars and implications for surface evolution. Science 284, 1495–1503.

Smith, D.E., Zuber, M.T., Neumann, G.A., 2001. Seasonal variations of snow depth on Mars. Science 294, 2141–2146.

Tillmann, J.E., 1988. Mars global atmospheric oscillations: annually synchronize, transient normal mode oscillations and the triggering of global dust storms. J. Geophys. Res. 93, 9433–9451.

Titus, T.N., Kieffer, H.H., Christensen, P.R., 2003. Exposed water ice discovered near the south pole of Mars. Science 299, 1048–1051.

Thomas, P.C., Malin, M.C., Edgett, K.S., Carr, M.H., Hartmann, W.K., Ingersoll, A.P., James, P.B., Soderblom, L.A., Veverka, J., Sullivan, R., 2000. North–south geological differences between the residual polar caps on Mars. Nature 404, 161–164.

Toon, O.B., Pollack, J.B., Ward, W., Burns, J.A., Biliski, K., 1980. The astronomical theory of climatic change on Mars. Icarus 44, 552–607.

Zurek, R.W., Barnes, J.R., Haberle, R.M., Pollack, J.B., Tillman, J.E., Leovy, C.B., 1992. Dynamics of the atmosphere of Mars. In: Kieffer, H.H., Jakosky, B.M., Snyder, C.W., Matthews, M.S. (Eds.), Mars. Univ. of Arizona Press, Tucson, pp. 835–932.